UNIVERSIDAD DE CONCEPCIÓN

Centro de Investigación en Ingeniería Matemática (CI^{2}MA)

Rotation-based mixed formulations for an elasticity-poroelasticity interface problem

Veronica Anaya, Zoa De Wijn,
Bryan Gomez-Vargas, David Mora,
Ricardo Ruiz-Baier

PREPRINT 2019-21

SERIE DE PRE-PUBLICACIONES

ROTATION-BASED MIXED FORMULATIONS FOR AN ELASTICITY-POROELASTICITY INTERFACE PROBLEM*

V. ANAYA†, Z. DE WIJN‡, B. GÓMEZ-VARGAS§, D. MORA¶, AND R. RUIZ-BAIER‖

Abstract. In this paper we introduce a new formulation for a stationary elasticity-poroelasticity problem written using rotations and total fluid-solid pressure as additional unknowns. The transmission conditions are imposed naturally in the weak formulation, and the analysis of the effective governing equations is conducted by an application of Fredholm's alternative. We also propose a monolithically coupled mixed finite element method for the numerical solution of the problem. Its convergence properties are rigorously derived, and subsequently confirmed by a set of computational tests that include applications to subsurface flow in reservoirs, and dentistry-oriented problems.

Key words. Elasticity - poroelasticity coupling; interface problems; Fredholm's alternative; mixed finite element method; error estimation.

AMS subject classifications. 65N30, 74A50, 76S05, 74F10.

1. Introduction.

The disparity of material properties across geometric interfaces is encountered in a wide variety of transmission problems arising in diverse scientific and engineering applications. This phenomenon is more clearly observed when the materials sharing the interface have intrinsically different features, such as an elastic medium in contact with a fluid or a poroleastic material in contact with an elastic one. For the latter, one specific example is the study of mechanical properties of the interaction between an oil reservoir and the surrounding non-pay rock. As mentioned in [13], the pore pressure variations and fluid content trapped in the cap rock are commonly not affected by outer injection or extraction of fluids in the reservoir. This fact motivates the use of partitioned models where in the reservoir one considers the classical Biot equations for poroelasticity, whereas the equations of linear elasticity suffice to describe the overall behaviour of the cap rock (see also [26]). In this case, a careful set up of interface conditions is required. We refer to [25, 21] for a detailed discussion on the physical and mathematical implications of these transmission terms.

Some other applications of coupling elastic-poroelastic systems include the reservoir modelling mentioned above, the classical problem of soil-structure interaction (soil-retaining walls and shallow foundations [20] or the earth's crustal deformation [23]), the simulation of periodontal ligament - tooth contact as done in [9], the development of noise reduction for aircraft design using acoustic-elastic wave propagation [17, 24], or the study of low-friction cartilage tissue in vertebrates [8].

The mathematical properties of this type of models have been addressed in [13]. There, the

*Funding: This work has been partially supported by CONICYT-Chile through FONDECYT project 11160706, through the Becas-Chile Programme for foreign students and through the project AFB170001 of the PIA Program: Concurso Apoyo a Centros Científicos y Tecnológicos de Excelencia con Financiamiento Basal; and by the Oxford Centre for Doctoral Training in Industrially Focused Mathematical Modelling.

†GIMNAP, Departamento de Matemática, Universidad del Bío-Bío, Concepción, Chile. E-mail: vanaya@ubiobio.cl.

‡Mathematical Institute, University of Oxford, Woodstock Road, Oxford OX2 6GG, UK. E-mail: dewijn@maths.ox.ac.uk.

§Sección de Matemática, Sede de Occidente, Universidad de Costa Rica, San Ramón, Costa Rica; and CI^{2}MA & Departamento de Ingeniería Matemática, Universidad de Concepción, Chile. E-mail: bryan.gomezvargas@ucr.ac.cr.

¶GIMNAP, Departamento de Matemática, Universidad del Bío-Bío, Concepción, Chile; and CI^{2}MA, Universidad de Concepción, Chile. E-mail: dmora@ubiobio.cl.

‖Corresponding author. Mathematical Institute, University of Oxford, Woodstock Road, Oxford OX2 6GG, UK. E-mail: ruizbaier@maths.ox.ac.uk.

authors develop a solvability theory for the semidiscrete elastic and poroelastic sub-problems, making use of a Galerkin method combined with compactness arguments permitting the passage to the limit.

In contrast, the specific version of the model we analyse here uses a modification of the recent displacement - rotation - pressure formulation of elasticity equations proposed in [2], together with a new formulation for the equations of poromechanics written in terms of displacement, fluid pressure, rotation, and total pressure. Our model assumes that the elastic domain is completely clamped on its exterior boundary, whereas on the interface between the poroelastic and elastic media we impose continuity of displacement, zero fluid flux, and a transmission condition related to the continuity of total traction forces written in terms of tangential rotations and pressure. It turns out from the mathematical structure of the set of equations and interface conditions that the system is written as a monolithic coupling, where the interface continuity conditions stated above are incorporated naturally through the weak formulation, without the need of additional Lagrange multipliers. In particular, the regularity of the displacement and the scaling of the momentum equations in both domains allows us to consider a global displacement. The well-posedness of the continuous problem is studied by grouping the unknowns with compatible regularity and realising that the resulting problem is a mixed variational formulation that resembles the system introduced in [22] that describes the Biot equations in their displacement-pressure-total pressure formulation and which is analysed using Fredholm's alternative. Our analysis also discusses the limit case when the specific storage coefficient in the poroelastic domain goes to zero, and we observe that the continuous dependence on data is robust with respect to the Lamé constants of the solids in both regions of the domain.

A similar framework is established for the discrete problem, here defined for Galerkin schemes with arbitrary order. For example we can employ piecewise quadratic and continuous approximations for displacements in the whole domain and for fluid pressure in the poroelastic medium; whereas piecewise linear and discontinuous approximations for all remaining unknowns (rotations in both domains, total pressure in the poroelastic domain, and solid pressure in the elastic domain). For this particular scheme our error estimates predict an overall second order accuracy, and the involved bounds are also robust with respect to the Lamé constants of the solids. Let us emphasise that the literature related to numerical methods for the coupling of elasticity and poroelasticity is still quite restricted. We are only aware of the conforming Galerkin scheme presented in [13], where a domain decomposition on the interface between the two subdomains is done by means of discontinuous Galerkin jumps and mortar terms; the stability of a mixed variant for that formulation, recently analysed in [15]; the primal method combined with stochastic parameter estimation advanced in [26]; and the loosely coupled segregated approaches developed for a fluid-poromechanics interaction problem studied in [5].

The contents of this paper will be presented in the following manner. Section 2 defines the model problem in strong form, specifying the boundary and interface conditions. It also includes the derivation of an appropriate weak formulation, and the statement of preliminary properties of the involved bilinear forms. The existence and uniqueness of weak solutions is then studied in section 3. This analysis is mainly based on Fredholm's alternative and saddle point theorems, where we also establish continuous dependence on data, with bounds that result robust with respect to the elasticity parameters intrinsic to each subdomain. A suitable Galerkin method together with finite element spaces will be defined in section 4. This section also incorporates the analysis of well-posedness of the discrete problem, the proof of a quasi-optimality result, and the derivation of a priori error bounds. We close in section 5 with a few computational examples that serve to confirm the accuracy of the mixed finite element method, and to illustrate the suitability of the model and of the family of schemes in some applicative problems.

2. Set of governing equations.

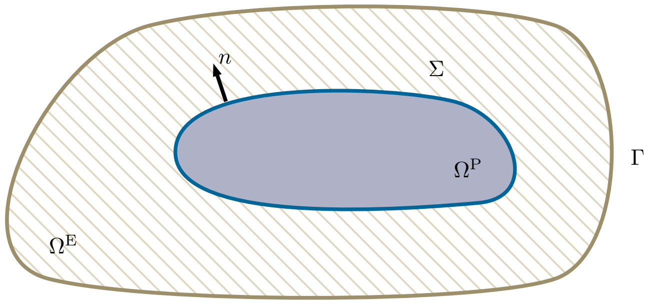

FIG. 1. *Sketch of the multidomain configuration.*

2.1. Model problem and boundary-transmission conditions. Let us consider a bounded Lipschitz domain $\Omega \subset \mathbb{R}^d$, $d \in \{2,3\}$, together with a partition into non-overlapping and connected subdomains $\Omega^{\rm E}$, $\Omega^{\rm P}$ representing zones of non-pay rock (where we will set the equations of linear elasticity) and a reservoir (where we aim at solving the poroelasticity equations), respectively. We also assume that the reservoir is completely immersed in the overall domain: $\overline{\Omega^{\rm P}} \subset \Omega$, such that the interface between the two subdomains, denoted as $\Sigma = \partial\Omega^{\rm P} \cap \partial\Omega^{\rm E}$, coincides with the boundary of the pay zone, as portrayed in Figure 1. Note that on the interface we consider that the normal unit vector $\boldsymbol{n}$ is pointing from $\Omega^{\rm P}$ to $\Omega^{\rm E}$.

In the reservoir we consider the following balance laws for the poroelasticity equations (see, for instance, [3]): find the displacement $\boldsymbol{u}^{\rm P}$ and the pore pressure of the fluid $p^{\rm P}$ such that

$$-\mu^{\rm P}\Delta\boldsymbol{u}^{\rm P} - (\lambda^{\rm P}+\mu^{\rm P})\nabla\,\mathrm{div}(\boldsymbol{u}^{\rm P}) + \alpha\nabla p^{\rm P} = \widetilde{\boldsymbol{f}}^{\rm P} \qquad \text{in } \Omega^{\rm P}, \tag{2.1}$$

$$c_0 p^{\rm P} + \alpha\,\mathrm{div}(\boldsymbol{u}^{\rm P}) - \frac{1}{\xi}\,\mathrm{div}\left[\kappa(\nabla p^{\rm P} - \rho\boldsymbol{g})\right] = s^{\rm P} \qquad \text{in } \Omega^{\rm P}, \tag{2.2}$$

where κ is the permeability of the porous matrix constituting the reservoir (here assumed isotropic and satisfying $0 < \kappa_1 \le \kappa(\boldsymbol{x}) \le \kappa_2 < \infty$, for all $\boldsymbol{x} \in \Omega^{\rm P}$), $\lambda^{\rm P}, \mu^{\rm P}$ are the Lamé constants of the solid $\Omega^{\rm P}$ (dilation and shear moduli of elasticity, respectively), $c_0 > 0$ is the constrained specific storage coefficient, $\alpha > 0$ is the Biot-Willis parameter, $\boldsymbol{g}$ is the gravity acceleration, and $\xi > 0, \rho > 0$ are the viscosity and density of the pore fluid, respectively. Next, for the poroelasticity problem, we propose a new four-field variational formulation. In fact, we begin by introducing the following additional unknowns

$$\phi^{\rm P} := \alpha(\lambda^{\rm P}+\mu^{\rm P})^{-1}p^{\rm P} - (1+\eta^{\rm P})\,\mathrm{div}(\boldsymbol{u}^{\rm P}) \quad \text{and} \quad \boldsymbol{\omega}^{\rm P} := \sqrt{\eta^{\rm P}}\,\mathbf{curl}\,\boldsymbol{u}^{\rm P}, \tag{2.3}$$

where the first one can be regarded as a rescaled total pressure or volumetric stress and the second one corresponds to the rescaled rotations, with the auxiliary scaling parameter $\eta^{\rm P} := \frac{\mu^{\rm P}}{\lambda^{\rm P}+\mu^{\rm P}}$. In this way, the identities in (2.3) in combination with (2.1)-(2.2) in turn gives rise to the following four-field formulation for the poroelasticity problem: find the displacement $\boldsymbol{u}^{\rm P}$, the poroelastic rotation vector $\boldsymbol{\omega}^{\rm P}$, the pore fluid pressure $p^{\rm P}$, and the rescaled total poroelastic pressure $\phi^{\rm P}$ such that

$$\sqrt{\eta^{\rm P}}\,\mathbf{curl}\,\boldsymbol{\omega}^{\rm P} + \nabla\phi^{\rm P} = \boldsymbol{f}^{\rm P} \qquad \text{in } \Omega^{\rm P}, \tag{2.4}$$

$$\boldsymbol{\omega}^{\rm P} - \sqrt{\eta^{\rm P}}\,\mathbf{curl}\,\boldsymbol{u}^{\rm P} = \mathbf{0} \qquad \text{in } \Omega^{\rm P}, \tag{2.5}$$

$$(1+\eta^{\rm P})^{-1}\phi^{\rm P} + \mathrm{div}(\boldsymbol{u}^{\rm P}) - \alpha(1+\eta^{\rm P})^{-1}(\lambda^{\rm P}+\mu^{\rm P})^{-1}p^{\rm P} = 0 \qquad \text{in } \Omega^{\rm P}, \tag{2.6}$$

$$\left[c_0 + \alpha^2(\mu^{\rm P}+\lambda^{\rm P})^{-1}(1+\eta^{\rm P})^{-1}\right]p^{\rm P} - \alpha(1+\eta^{\rm P})^{-1}\phi^{\rm P} - \frac{1}{\xi}\,\mathrm{div}\left[\kappa(\nabla p^{\rm P} - \rho\boldsymbol{g})\right] = s^{\rm P} \qquad \text{in } \Omega^{\rm P}, \tag{2.7}$$

where the right-hand side has been rescaled as $\boldsymbol{f}^{\mathrm{P}} := \frac{1}{\lambda^{\mathrm{P}}+\mu^{\mathrm{P}}}\widetilde{\boldsymbol{f}}^{\mathrm{P}}$.

In Ω^{E} the governing equations correspond to the system of linear elasticity written in terms of displacement $\boldsymbol{u}^{\mathrm{E}}$, elastic pressure p^{E}, and elastic rotation vector $\boldsymbol{\omega}^{\mathrm{E}} := \sqrt{\eta^{\mathrm{E}}}\,\mathbf{curl}\,\boldsymbol{u}^{\mathrm{E}}$ associated with the non-pay zone:

$$\sqrt{\eta^{\mathrm{E}}}\,\mathbf{curl}\,\boldsymbol{\omega}^{\mathrm{E}} + \nabla p^{\mathrm{E}} = \boldsymbol{f}^{\mathrm{E}} \quad \text{in } \Omega^{\mathrm{E}}, \tag{2.8}$$

$$\boldsymbol{\omega}^{\mathrm{E}} - \sqrt{\eta^{\mathrm{E}}}\,\mathbf{curl}\,\boldsymbol{u}^{\mathrm{E}} = 0 \quad \text{in } \Omega^{\mathrm{E}}, \tag{2.9}$$

$$\operatorname{div}\boldsymbol{u}^{\mathrm{E}} + p^{\mathrm{E}} = 0 \quad \text{in } \Omega^{\mathrm{E}}, \tag{2.10}$$

where $\eta^{\mathrm{E}} := \frac{\mu^{\mathrm{E}}}{2\mu^{\mathrm{E}}+\lambda^{\mathrm{E}}} > 0$ is a scaling parameter depending on the Lamé constants of the elastic non-pay rock Ω^{E}, and $\boldsymbol{f}^{\mathrm{E}}$ corresponds to the rescaled function $\boldsymbol{f}^{\mathrm{E}} := \frac{1}{2\mu^{\mathrm{E}}+\lambda^{\mathrm{E}}}\widetilde{\boldsymbol{f}}^{\mathrm{E}}$. Note that the scaling is different than the one used in the formulation proposed in [2].

We assume here that on the external boundary of the non-pay rock the displacements are zero

$$\boldsymbol{u}^{\mathrm{E}} = \mathbf{0} \quad \text{on} \quad \Gamma, \tag{2.11}$$

and the system is closed by setting suitable transmission conditions on the interface between the reservoir and the non-pay zone

$$\boldsymbol{u}^{\mathrm{P}} = \boldsymbol{u}^{\mathrm{E}}, \quad \sqrt{\eta^{\mathrm{P}}}\,\boldsymbol{\omega}^{\mathrm{P}} \times \boldsymbol{n} + \phi^{\mathrm{P}}\boldsymbol{n} = \sqrt{\eta^{\mathrm{E}}}\,\boldsymbol{\omega}^{\mathrm{E}} \times \boldsymbol{n} + p^{\mathrm{E}}\boldsymbol{n}, \quad \frac{\kappa}{\xi}(\nabla p^{\mathrm{P}} - \rho\boldsymbol{g})\cdot\boldsymbol{n} = 0, \quad \text{on} \quad \Sigma, \tag{2.12}$$

which represent continuity of the medium, a generalised relation for the matching of total normal stresses, and no-flux of fluid at the interface, respectively. The second condition in equation (2.12) can be linked to the generalised Navier condition used in fluids

$$[\boldsymbol{\epsilon}(\boldsymbol{u}^{\mathrm{P}})\boldsymbol{n}]_\tau + \Lambda\boldsymbol{u}^{\mathrm{P}} = \mathbf{0},$$

where the subscript τ denotes the vectorial tangential trace of any vector, defined by $\boldsymbol{v}_\tau := \boldsymbol{v} - (\boldsymbol{v}\cdot\boldsymbol{n})\boldsymbol{n}$, and Λ is a type (1,1) tensor defined on Σ [12]. In the simple case when $\Lambda = \delta\mathbf{I}$ (with δ a positive or negative friction coefficient), then one retrieves a Navier-type friction transmission condition. If Λ is instead the Weingarten shape operator on the interface, this results in a continuity condition for the tangential rotations and the normal total pressure. Similar ideas can be found in e.g. [12, 1, 7, 18, 6, 25] for Navier-Stokes/Darcy, Brinkman-Darcy couplings, vascular Stokes-Darcy models, Lagrangian-Eulerian fluid-elastic transmission, time-harmonic elastic waves, and interface poromechanics, respectively. The last transmission condition imposes no leakage between the bodies as they are compressed, which implies mass conservation [8].

2.2. Weak formulation. In order to derive a weak formulation for the system (2.4)-(2.12), we start by multiplying each equation of the poroelasticity problem by suitable test functions, integrating by parts whenever adequate (see (2.15)-(2.16) below) and applying the second and third transmission condition given in (2.12) to obtain:

$$-\sqrt{\eta^{\mathrm{P}}}\int_{\Omega^{\mathrm{P}}}\mathbf{curl}\,\boldsymbol{v}^{\mathrm{P}}\cdot\boldsymbol{\omega}^{\mathrm{P}} + \int_{\Omega^{\mathrm{P}}}\phi^{\mathrm{P}}\operatorname{div}(\boldsymbol{v}^{\mathrm{P}}) - \langle\sqrt{\eta^{\mathrm{E}}}\,\boldsymbol{\omega}^{\mathrm{E}}\times\boldsymbol{n} + p^{\mathrm{E}}\boldsymbol{n}, \boldsymbol{v}^{\mathrm{P}}\rangle_\Sigma = -\int_{\Omega^{\mathrm{P}}}\boldsymbol{f}^{\mathrm{P}}\cdot\boldsymbol{v}^{\mathrm{P}},$$

$$\int_{\Omega^{\mathrm{P}}}\boldsymbol{\omega}^{\mathrm{P}}\cdot\boldsymbol{\theta}^{\mathrm{P}} - \sqrt{\eta^{\mathrm{P}}}\int_{\Omega^{\mathrm{P}}}\boldsymbol{\theta}^{\mathrm{P}}\cdot\mathbf{curl}\,\boldsymbol{u}^{\mathrm{P}} = 0,$$

(2.13)

$$(1+\eta^{\mathrm{P}})^{-1}\int_{\Omega^{\mathrm{P}}}\phi^{\mathrm{P}}\psi^{\mathrm{P}} + \int_{\Omega^{\mathrm{P}}}\psi^{\mathrm{P}}\operatorname{div}(\boldsymbol{u}^{\mathrm{P}}) - \alpha(1+\eta^{\mathrm{P}})^{-1}(\lambda^{\mathrm{P}}+\mu^{\mathrm{P}})^{-1}\int_{\Omega^{\mathrm{P}}}p^{\mathrm{P}}\psi^{\mathrm{P}} = 0,$$

$$- \left[c_0 + \alpha^2(\mu^{\mathrm{P}} + \lambda^{\mathrm{P}})^{-1}(1+\eta^{\mathrm{P}})^{-1}\right] \int_{\Omega^{\mathrm{P}}} p^{\mathrm{P}} q^{\mathrm{P}} + \alpha(1+\eta^{\mathrm{P}})^{-1} \int_{\Omega^{\mathrm{P}}} \phi^{\mathrm{P}} q^{\mathrm{P}} - \xi^{-1} \int_{\Omega^{\mathrm{P}}} \kappa \nabla p^{\mathrm{P}} \cdot \nabla q^{\mathrm{P}}$$
$$= -\rho\xi^{-1} \int_{\Omega^{\mathrm{P}}} \kappa \boldsymbol{g} \cdot \nabla q^{\mathrm{P}} - \int_{\Omega^{\mathrm{P}}} s^{\mathrm{P}} q^{\mathrm{P}},$$

for each $(\boldsymbol{v}^{\mathrm{P}}, \boldsymbol{\theta}^{\mathrm{P}}, \psi^{\mathrm{P}}, q^{\mathrm{P}}) \in \mathbf{H}^1(\Omega^{\mathrm{P}}) \times \mathbf{L}^2(\Omega^{\mathrm{P}}) \times \mathrm{L}^2(\Omega^{\mathrm{P}}) \times \mathrm{H}^1(\Omega^{\mathrm{P}})$. In turn, for (2.8)-(2.10) we proceed as in the mixed displacement-rotation-pressure formulation for linear elasticity introduced in [2], and we obtain:

$$\begin{aligned} -\sqrt{\eta^{\mathrm{E}}} \int_{\Omega^{\mathrm{E}}} \boldsymbol{\omega}^{\mathrm{E}} \cdot \mathbf{curl}\, \boldsymbol{v}^{\mathrm{E}} + \int_{\Omega^{\mathrm{E}}} p^{\mathrm{E}} \operatorname{div}(\boldsymbol{v}^{\mathrm{E}}) + \langle \sqrt{\eta^{\mathrm{E}}}\, \boldsymbol{\omega}^{\mathrm{E}} \times \boldsymbol{n} + p^{\mathrm{E}} \boldsymbol{n}, \boldsymbol{v}^{\mathrm{E}} \rangle_{\Sigma} &= -\int_{\Omega^{\mathrm{E}}} \boldsymbol{f}^{\mathrm{E}} \cdot \boldsymbol{v}^{\mathrm{E}}, \\ \int_{\Omega^{\mathrm{E}}} \boldsymbol{\omega}^{\mathrm{E}} \cdot \boldsymbol{\theta}^{\mathrm{E}} - \sqrt{\eta^{\mathrm{E}}} \int_{\Omega^{\mathrm{E}}} \boldsymbol{\theta}^{\mathrm{E}} \cdot \mathbf{curl}\, \boldsymbol{u}^{\mathrm{E}} &= 0, \\ \int_{\Omega^{\mathrm{E}}} q^{\mathrm{E}} \operatorname{div}(\boldsymbol{u}^{\mathrm{E}}) + \int_{\Omega^{\mathrm{E}}} p^{\mathrm{E}} q^{\mathrm{E}} &= 0, \end{aligned} \tag{2.14}$$

for each $(\boldsymbol{v}^{\mathrm{E}}, \boldsymbol{\theta}^{\mathrm{E}}, q^{\mathrm{E}}) \in \mathbf{H}^1_\Gamma(\Omega^{\mathrm{E}}) \times \mathbf{L}^2(\Omega^{\mathrm{E}}) \times \mathrm{L}^2(\Omega^{\mathrm{E}})$, where

$$\mathbf{H}^1_\Gamma(\Omega^{\mathrm{E}}) := \{\boldsymbol{v}^{\mathrm{E}} \in \mathbf{H}^1(\Omega^{\mathrm{E}}) : \quad \boldsymbol{v}^{\mathrm{E}} = \mathbf{0} \quad \text{on} \quad \Gamma\}.$$

Recall that, according to [14, Theorem 2.11], for a generic domain Ω, the relevant integration by parts formula corresponds to

$$\int_\Omega \mathbf{curl}\, \boldsymbol{\omega} \cdot \boldsymbol{v} = \int_\Omega \boldsymbol{\omega} \cdot \mathbf{curl}\, \boldsymbol{v} + \langle \boldsymbol{\omega} \times \boldsymbol{n}, \boldsymbol{v} \rangle_{\partial\Omega}, \tag{2.15}$$

if $\Omega \subseteq \mathbb{R}^3$, or to

$$\int_\Omega \mathbf{curl}\, \omega \cdot \boldsymbol{v} = \int_\Omega \omega \operatorname{rot} \boldsymbol{v} - \langle \boldsymbol{v} \cdot \boldsymbol{t}, \omega \rangle_{\partial\Omega}, \tag{2.16}$$

in 2D, where $\boldsymbol{t}$ is the tangent vector.

The first transmission condition in (2.12) together with the regularity of the solid displacements on each subdomain (to be specified below), imply that we can consider a single displacement field $\boldsymbol{u}$ and test function $\boldsymbol{v}$. That is the reason why the duality pairings between $\mathrm{H}^{-1/2}(\Sigma)$ and $\mathrm{H}^{1/2}(\Sigma)$ (represented by $\langle \cdot, \cdot \rangle_\Sigma$) disappear when we add the first row in (2.14) to the first row in (2.13). Furthermore, from now on we regard the poroelastic and elastic rotation vectors $\boldsymbol{\omega}^{\mathrm{P}}$ and $\boldsymbol{\omega}^{\mathrm{E}}$, respectively, the rescaled total poroelastic pressure ϕ^{P}, and the pressure p^{E} in the elastic domain as a single auxiliary unknown, namely $\vec{\boldsymbol{\omega}} := (\boldsymbol{\omega}^{\mathrm{P}}, \phi^{\mathrm{P}}, \boldsymbol{\omega}^{\mathrm{E}}, p^{\mathrm{E}})$ (defined in an appropriate product functional space), such that we can establish the well-posedness of the mixed variational formulation of interest using the Fredholm's alternative theory for compact operators. Under this assumption, we arrive at: find $(\vec{\boldsymbol{\omega}}, \boldsymbol{u}, p^{\mathrm{P}}) \in \mathbf{H} \times \mathbf{V} \times \mathrm{Q}^{\mathrm{P}}$ such that

$$a(\vec{\boldsymbol{\omega}}, \vec{\boldsymbol{\theta}}) + b_1(\vec{\boldsymbol{\theta}}, \boldsymbol{u}) - b_2(\vec{\boldsymbol{\theta}}, p^{\mathrm{P}}) = 0 \qquad \forall\, \vec{\boldsymbol{\theta}} \in \mathbf{H}, \tag{2.17}$$
$$b_1(\vec{\boldsymbol{\omega}}, \boldsymbol{v}) = F(\boldsymbol{v}) \qquad \forall\, \boldsymbol{v} \in \mathbf{V}, \tag{2.18}$$
$$b_3(\vec{\boldsymbol{\omega}}, q^{\mathrm{P}}) - c(p^{\mathrm{P}}, q^{\mathrm{P}}) = G(q^{\mathrm{P}}) \qquad \forall\, q^{\mathrm{P}} \in \mathrm{Q}^{\mathrm{P}}, \tag{2.19}$$

where the vector $\vec{\boldsymbol{\theta}} := (\boldsymbol{\theta}^{\mathrm{P}}, \psi^{\mathrm{P}}, \boldsymbol{\theta}^{\mathrm{E}}, q^{\mathrm{E}})$, and the boundary and interface conditions suggest to define the involved functional spaces as

$$\mathbf{H} := \mathbf{L}^2(\Omega^{\mathrm{P}}) \times \mathrm{L}^2(\Omega^{\mathrm{P}}) \times \mathbf{L}^2(\Omega^{\mathrm{E}}) \times \mathrm{L}^2(\Omega^{\mathrm{E}}), \quad \mathbf{V} := \mathbf{H}^1_0(\Omega), \quad \mathrm{Q}^{\mathrm{P}} := \mathrm{H}^1(\Omega^{\mathrm{P}}),$$

and the bilinear forms $a : \mathbf{H} \times \mathbf{H} \to \mathbb{R}$, $b_1 : \mathbf{H} \times \mathbf{V} \to \mathbb{R}$, $b_2 : \mathbf{H} \times \mathrm{Q}^{\mathrm{P}} \to \mathbb{R}$, $b_3 : \mathbf{H} \times \mathrm{Q}^{\mathrm{P}} \to \mathbb{R}$, $c : \mathrm{Q}^{\mathrm{P}} \times \mathrm{Q}^{\mathrm{P}} \to \mathbb{R}$, and linear functionals $F : \mathbf{V} \to \mathbb{R}$, $G : \mathrm{Q}^{\mathrm{P}} \to \mathbb{R}$ are specified in the following way

$$a(\vec{\boldsymbol{\omega}}, \vec{\boldsymbol{\theta}}) := \int_{\Omega^{\mathrm{P}}} \boldsymbol{\omega}^{\mathrm{P}} \cdot \boldsymbol{\theta}^{\mathrm{P}} + \frac{1}{1+\eta^{\mathrm{P}}} \int_{\Omega^{\mathrm{P}}} \phi^{\mathrm{P}} \psi^{\mathrm{P}} + \int_{\Omega^{\mathrm{E}}} \boldsymbol{\omega}^{\mathrm{E}} \cdot \boldsymbol{\theta}^{\mathrm{E}} + \int_{\Omega^{\mathrm{E}}} p^{\mathrm{E}} q^{\mathrm{E}},$$

$$\begin{aligned}
b_1(\vec{\boldsymbol{\theta}},\boldsymbol{v}) &:= -\sqrt{\eta^{\mathrm{P}}}\int_{\Omega^{\mathrm{P}}}\boldsymbol{\theta}^{\mathrm{P}}\cdot\mathbf{curl}\,\boldsymbol{v} + \int_{\Omega^{\mathrm{P}}}\psi^{\mathrm{P}}\operatorname{div}\boldsymbol{v} - \sqrt{\eta^{\mathrm{E}}}\int_{\Omega^{\mathrm{E}}}\boldsymbol{\theta}^{\mathrm{E}}\cdot\mathbf{curl}\,\boldsymbol{v} + \int_{\Omega^{\mathrm{E}}}q^{\mathrm{E}}\operatorname{div}\boldsymbol{v},\\
b_2(\vec{\boldsymbol{\theta}},p^{\mathrm{P}}) &:= \frac{\alpha}{(1+\eta^{\mathrm{P}})(\lambda^{\mathrm{P}}+\mu^{\mathrm{P}})}\int_{\Omega^{\mathrm{P}}}p^{\mathrm{P}}\psi^{\mathrm{P}}, \qquad b_3(\vec{\boldsymbol{\omega}},q^{\mathrm{P}}) := \frac{\alpha}{(1+\eta^{\mathrm{P}})}\int_{\Omega^{\mathrm{P}}}q^{\mathrm{P}}\phi^{\mathrm{P}},\\
c(p^{\mathrm{P}},q^{\mathrm{P}}) &:= \left[c_0 + \frac{\alpha^2}{(\mu^{\mathrm{P}}+\lambda^{\mathrm{P}})(1+\eta^{\mathrm{P}})}\right]\int_{\Omega^{\mathrm{P}}}p^{\mathrm{P}}q^{\mathrm{P}} + \frac{1}{\xi}\int_{\Omega^{\mathrm{P}}}\kappa\nabla p^{\mathrm{P}}\cdot\nabla q^{\mathrm{P}},\\
F(\boldsymbol{v}) &:= -\int_{\Omega^{\mathrm{P}}}\boldsymbol{f}^{\mathrm{P}}\cdot\boldsymbol{v} - \int_{\Omega^{\mathrm{E}}}\boldsymbol{f}^{\mathrm{E}}\cdot\boldsymbol{v}, \qquad G(q^{\mathrm{P}}) := -\frac{\rho}{\xi}\int_{\Omega^{\mathrm{P}}}\kappa\boldsymbol{g}\cdot\nabla q^{\mathrm{P}} - \int_{\Omega^{\mathrm{P}}}s^{\mathrm{P}}q^{\mathrm{P}}.
\end{aligned}$$

For the forthcoming analysis, we will consider the following η^{P} and $\eta^{\mathrm{E}}-$dependent norms (see for instance, [14, Remark 2.7]) for the displacements on the solid and elastic domains Ω^{P} and Ω^{E}, respectively:

$$\|\boldsymbol{v}\|^2_{\mathbf{V}^{\mathrm{P}}} := \eta^{\mathrm{P}}\|\,\mathbf{curl}\,\boldsymbol{v}\|^2_{0,\Omega^{\mathrm{P}}} + \|\operatorname{div}\boldsymbol{v}\|^2_{0,\Omega^{\mathrm{P}}} \quad\text{and}\quad \|\boldsymbol{v}\|^2_{\mathbf{V}^{\mathrm{E}}} := \eta^{\mathrm{E}}\|\,\mathbf{curl}\,\boldsymbol{v}\|^2_{0,\Omega^{\mathrm{E}}} + \|\operatorname{div}\boldsymbol{v}\|^2_{0,\Omega^{\mathrm{E}}},$$

which in turn give rise to the following η^{P} and $\eta^{\mathrm{E}}-$dependent norm on the space $\mathbf{V}$:

$$\|\boldsymbol{v}\|^2_{\mathbf{V}} := \|\boldsymbol{v}\|^2_{\mathbf{V}^{\mathrm{P}}} + \|\boldsymbol{v}\|^2_{\mathbf{V}^{\mathrm{E}}}.$$

Moreover, $\mathbf{H}$ will be endowed with the norm

$$\|\vec{\boldsymbol{\theta}}\|^2_{\mathbf{H}} := \|\boldsymbol{\theta}^{\mathrm{P}}\|^2_{0,\Omega^{\mathrm{P}}} + \|\psi^{\mathrm{P}}\|^2_{0,\Omega^{\mathrm{P}}} + \|\boldsymbol{\theta}^{\mathrm{E}}\|^2_{0,\Omega^{\mathrm{E}}} + \|q^{\mathrm{E}}\|^2_{0,\Omega^{\mathrm{E}}}.$$

3. Well-posedness analysis. Before addressing the well-posedness of the continuous formulation, we indicate that the bilinear forms and the linear functionals appearing in the variational problem of interest are all bounded by constants independent of η^{P} and η^{E} (see, for instance, [2]). We also recall the positivity of the bilinear forms $a(\cdot,\cdot)$, and $c(\cdot,\cdot)$

$$\begin{aligned}
a(\vec{\boldsymbol{\theta}},\vec{\boldsymbol{\theta}}) &\geq \frac{1}{(1+\eta^{\mathrm{P}})}\|\vec{\boldsymbol{\theta}}\|^2_{\mathbf{H}} \qquad \forall\,\vec{\boldsymbol{\theta}}\in\mathbf{H},\\
c(q^{\mathrm{P}},q^{\mathrm{P}}) &\geq \left[c_0 + \frac{\alpha^2}{(\mu^{\mathrm{P}}+\lambda^{\mathrm{P}})(1+\eta^{\mathrm{P}})}\right]\|q^{\mathrm{P}}\|_{0,\Omega^{\mathrm{P}}} + \frac{\kappa_1}{\xi}|q^{\mathrm{P}}|_{1,\Omega^{\mathrm{P}}} \qquad \forall\,q^{\mathrm{P}}\in \mathrm{Q}^{\mathrm{P}};
\end{aligned}$$

as well as the continuous inf-sup condition satisfied by $b_1(\cdot,\cdot)$, stated in the following result.

LEMMA 3.1. *There exists $\beta>0$, independent of η^{P} and η^{E}, such that*

$$\sup_{\vec{\boldsymbol{\theta}}\in\mathbf{H}\setminus\mathbf{0}}\frac{b_1(\vec{\boldsymbol{\theta}},\boldsymbol{v})}{\|\vec{\boldsymbol{\theta}}\|_{\mathbf{H}}} \geq \beta\|\boldsymbol{v}\|_{\mathbf{V}} \qquad \forall\,\boldsymbol{v}\in\mathbf{V}. \tag{3.1}$$

Proof. Proceeding similarly as in [2, Lemma 2.2], let us consider an arbitrary $\boldsymbol{v}\in\mathbf{V}$ and define

$$\vec{\boldsymbol{\theta}}_\beta := (-\sqrt{\eta^{\mathrm{P}}}\,\mathbf{curl}\,\boldsymbol{v}|_{\Omega^{\mathrm{P}}}, \operatorname{div}(\boldsymbol{v})|_{\Omega^{\mathrm{P}}}, -\sqrt{\eta^{\mathrm{E}}}\,\mathbf{curl}\,\boldsymbol{v}|_{\Omega^{\mathrm{E}}}, \operatorname{div}(\boldsymbol{v})|_{\Omega^{\mathrm{E}}}) \in \mathbf{H}.$$

In this way, noting that

$$\|\vec{\boldsymbol{\theta}}_\beta\|_{\mathbf{H}} \leq \|\boldsymbol{v}\|_{\mathbf{V}},$$

and using the definition of $b_1(\cdot,\cdot)$, we readily obtain

$$\sup_{\vec{\boldsymbol{\theta}}\in\mathbf{H}\setminus\mathbf{0}}\frac{b_1(\vec{\boldsymbol{\theta}},\boldsymbol{v})}{\|\vec{\boldsymbol{\theta}}\|_{\mathbf{H}}} \geq \frac{b_1(\vec{\boldsymbol{\theta}}_\beta,\boldsymbol{v})}{\|\vec{\boldsymbol{\theta}}_\beta\|_{\mathbf{H}}} \geq \beta\|\boldsymbol{v}\|_{\mathbf{V}} \qquad \forall\,\boldsymbol{v}\in\mathbf{H},$$

where we highlight that the constant β is strictly positive and independent of the auxiliary scaling parameters η^{P} and η^{E}. ∎

3.1. Stability. In this section we establish the stability of the problem by combining the boundedness, positivity, and inf-sup conditions from Section 2. We begin with the following result.

LEMMA 3.2. *Let* $(\vec{\boldsymbol{\omega}}, \boldsymbol{u}, p^{\mathrm{P}}) \in \mathbf{H}\times\mathbf{V}\times \mathrm{Q}^{\mathrm{P}}$ *be a solution of the system* (2.17)-(2.19)*, then there exists a constant* $C>0$*, independent of* η^{P} *and* η^{E}*, such that*

$$\|\vec{\boldsymbol{\omega}}\|_{\mathbf{H}} + \|\boldsymbol{u}\|_{\mathbf{V}} + \|p^{\mathrm{P}}\|_{1,\Omega^{\mathrm{P}}} \le C\big\{(\mu^{\mathrm{P}}+\lambda^{\mathrm{P}})(\|\boldsymbol{f}^{\mathrm{E}}\|_{0,\Omega^{\mathrm{E}}} + \|\boldsymbol{f}^{\mathrm{P}}\|_{0,\Omega^{\mathrm{P}}}) + \|\boldsymbol{g}\|_{0,\Omega^{\mathrm{P}}} + \|s^{\mathrm{P}}\|_{0,\Omega^{\mathrm{P}}}\big\}. \tag{3.2}$$

Proof. We start by considering $\vec{\boldsymbol{\theta}} = \vec{\boldsymbol{\omega}}$ in equation (2.17) and $\boldsymbol{v} = \boldsymbol{u}$ in equation (2.18). Thus, combining both equations, and applying the ellipticity of the bilinear form $a(\cdot,\cdot)$ we obtain

$$\frac{1}{1+\eta^{\mathrm{P}}}\|\vec{\boldsymbol{\omega}}\|_{\mathbf{H}}^2 \le a(\vec{\boldsymbol{\omega}},\vec{\boldsymbol{\omega}}) \le \frac{\alpha}{(1+\eta^{\mathrm{P}})(\mu^{\mathrm{P}}+\lambda^{\mathrm{P}})}\|\vec{\boldsymbol{\omega}}\|_{\mathbf{H}}\|p^{\mathrm{P}}\|_{0,\Omega^{\mathrm{P}}} + (\|\boldsymbol{f}^{\mathrm{P}}\|_{0,\Omega^{\mathrm{P}}} + \|\boldsymbol{f}^{\mathrm{E}}\|_{0,\Omega^{\mathrm{E}}})\|\boldsymbol{u}\|_{1,\Omega^{\mathrm{P}}}$$

which, by using classical Young's inequality, can be rewritten as

$$\frac{1}{2(1+\eta^{\mathrm{P}})}\|\vec{\boldsymbol{\omega}}\|_{\mathbf{H}}^2 \le \frac{\alpha^2}{2(1+\eta^{\mathrm{P}})(\mu^{\mathrm{P}}+\lambda^{\mathrm{P}})^2}\|p^{\mathrm{P}}\|_{0,\Omega^{\mathrm{P}}}^2 + (\|\boldsymbol{f}^{\mathrm{P}}\|_{0,\Omega^{\mathrm{P}}} + \|\boldsymbol{f}^{\mathrm{E}}\|_{0,\Omega^{\mathrm{E}}})\|\boldsymbol{u}\|_{0,\Omega^{\mathrm{P}}}, \tag{3.3}$$

or what is the same

$$\frac{(\mu^{\mathrm{P}}+\lambda^{\mathrm{P}})}{2(1+\eta^{\mathrm{P}})}\|\vec{\boldsymbol{\omega}}\|_{\mathbf{H}}^2 \le \frac{\alpha^2}{2(1+\eta^{\mathrm{P}})(\mu^{\mathrm{P}}+\lambda^{\mathrm{P}})}\|p^{\mathrm{P}}\|_{0,\Omega^{\mathrm{P}}}^2 + (\mu^{\mathrm{P}}+\lambda^{\mathrm{P}})(\|\boldsymbol{f}^{\mathrm{P}}\|_{0,\Omega^{\mathrm{P}}} + \|\boldsymbol{f}^{\mathrm{E}}\|_{0,\Omega^{\mathrm{E}}})\|\boldsymbol{u}\|_{0,\Omega^{\mathrm{P}}}. \tag{3.4}$$

Furthermore, choosing $q^{\mathrm{P}} = p^{\mathrm{P}}$ in (2.19), and applying the positivity of $c(\cdot,\cdot)$, we get

$$\begin{aligned}\left[c_0 + \frac{\alpha^2}{(\mu^{\mathrm{P}}+\lambda^{\mathrm{P}})(1+\eta^{\mathrm{P}})}\right]\|p^{\mathrm{P}}\|_{0,\Omega^{\mathrm{P}}}^2 + \frac{\kappa_1}{\xi}|p^{\mathrm{P}}|_{1,\Omega^{\mathrm{P}}}^2 \\ \le \frac{\alpha}{1+\eta^{\mathrm{P}}}\|\vec{\boldsymbol{\omega}}\|_{\mathbf{H}}\|p^{\mathrm{P}}\|_{0,\Omega^{\mathrm{P}}} + (\rho\xi^{-1}\kappa_2\|\boldsymbol{g}\|_{0,\Omega^{\mathrm{P}}} + \|s^{\mathrm{P}}\|_{0,\Omega^{\mathrm{P}}})\|p^{\mathrm{P}}\|_{1,\Omega^{\mathrm{P}}},\end{aligned} \tag{3.5}$$

such that applying Young's inequality with constant $\delta := \frac{\mu^{\mathrm{P}}+\lambda^{\mathrm{P}}}{\alpha}$ to the first term on the right-hand side of (3.5) and then using (3.4) gives

$$\begin{aligned}\left[c_0 + \frac{\alpha^2}{(\mu^{\mathrm{P}}+\lambda^{\mathrm{P}})(1+\eta^{\mathrm{P}})}\right]\|p^{\mathrm{P}}\|_{0,\Omega^{\mathrm{P}}}^2 + \frac{\kappa_1}{\xi}|p^{\mathrm{P}}|_{1,\Omega^{\mathrm{P}}}^2 \le \frac{\alpha^2}{(\mu^{\mathrm{P}}+\lambda^{\mathrm{P}})(1+\eta^{\mathrm{P}})}\|p^{\mathrm{P}}\|_{0,\Omega^{\mathrm{P}}}^2 \\ + (\mu^{\mathrm{P}}+\lambda^{\mathrm{P}})(\|\boldsymbol{f}^{\mathrm{P}}\|_{0,\Omega^{\mathrm{P}}} + \|\boldsymbol{f}^{\mathrm{E}}\|_{0,\Omega^{\mathrm{E}}})\|\boldsymbol{u}\|_{1,\Omega^{\mathrm{P}}} + (\rho\xi^{-1}\kappa_2\|\boldsymbol{g}\|_{0,\Omega^{\mathrm{P}}} + \|s^{\mathrm{P}}\|_{0,\Omega^{\mathrm{P}}})\|p^{\mathrm{P}}\|_{1,\Omega^{\mathrm{P}}},\end{aligned}$$

or what is the same

$$c_1\|p^{\mathrm{P}}\|_{1,\Omega^{\mathrm{P}}}^2 \le (\mu^{\mathrm{P}}+\lambda^{\mathrm{P}})(\|\boldsymbol{f}^{\mathrm{P}}\|_{0,\Omega^{\mathrm{P}}} + \|\boldsymbol{f}^{\mathrm{E}}\|_{0,\Omega^{\mathrm{E}}})\|\boldsymbol{u}\|_{1,\Omega^{\mathrm{P}}} + (\rho\xi^{-1}\kappa_2\|\boldsymbol{g}\|_{0,\Omega^{\mathrm{P}}} + \|s^{\mathrm{P}}\|_{0,\Omega^{\mathrm{P}}})\|p^{\mathrm{P}}\|_{1,\Omega^{\mathrm{P}}}, \tag{3.6}$$

where $c_1 := \min\{c_0, \kappa_1\xi^{-1}\}$. On the other hand, by combining (3.3) and (3.5), we obtain

$$\begin{aligned}\frac{1}{1+\eta^{\mathrm{P}}}\|\vec{\boldsymbol{\omega}}\|_{\mathbf{H}}^2 \le \frac{\alpha}{1+\eta^{\mathrm{P}}}\|\vec{\boldsymbol{\omega}}\|_{\mathbf{H}}\|p^{\mathrm{P}}\|_{0,\Omega^{\mathrm{P}}} \\ + 2(\|\boldsymbol{f}^{\mathrm{P}}\|_{0,\Omega^{\mathrm{P}}} + \|\boldsymbol{f}^{\mathrm{P}}\|_{0,\Omega^{\mathrm{E}}})\|\boldsymbol{u}\|_{1,\Omega^{\mathrm{P}}} + (\rho\xi^{-1}\kappa_2\|\boldsymbol{g}\|_{0,\Omega^{\mathrm{P}}} + \|s^{\mathrm{P}}\|_{0,\Omega^{\mathrm{P}}})\|p^{\mathrm{P}}\|_{1,\Omega^{\mathrm{P}}},\end{aligned}$$

which, applying Young's inequality leads to

$$\begin{aligned}\frac{1}{2(1+\eta^{\mathrm{P}})}\|\vec{\boldsymbol{\omega}}\|_{\mathbf{H}}^2 \le \frac{\alpha^2}{2(1+\eta^{\mathrm{P}})}\|p^{\mathrm{P}}\|_{0,\Omega^{\mathrm{P}}}^2 \\ + 2(\|\boldsymbol{f}^{\mathrm{P}}\|_{0,\Omega^{\mathrm{P}}} + \|\boldsymbol{f}^{\mathrm{P}}\|_{0,\Omega^{\mathrm{E}}})\|\boldsymbol{u}\|_{1,\Omega^{\mathrm{P}}} + (\rho\xi^{-1}\kappa_2\|\boldsymbol{g}\|_{0,\Omega^{\mathrm{P}}} + \|s^{\mathrm{P}}\|_{0,\Omega^{\mathrm{P}}})\|p^{\mathrm{P}}\|_{1,\Omega^{\mathrm{P}}}.\end{aligned} \tag{3.7}$$

Now, from the inf-sup condition (3.1) with $\boldsymbol{v} = \boldsymbol{u}$ and using (2.17), we get

$$\beta \|\boldsymbol{u}\|_{\mathbf{V}} \leq \frac{\alpha}{(\mu^{\mathrm{P}} + \lambda^{\mathrm{P}})(1 + \eta^{\mathrm{P}})} \|p^{\mathrm{P}}\|_{0,\Omega^{\mathrm{P}}} + \|\vec{\boldsymbol{\omega}}\|_{\mathbf{H}}. \tag{3.8}$$

Finally, substituting (3.8) back into (3.6) and (3.7), and then applying Young's inequality whenever adequate, we obtain the desired result. □

Remark 3.1. *The expression* $(\mu^{\mathrm{P}} + \lambda^{\mathrm{P}})(\|\boldsymbol{f}^{\mathrm{E}}\|_{0,\Omega^{\mathrm{E}}} + \|\boldsymbol{f}^{\mathrm{P}}\|_{0,\Omega^{\mathrm{P}}})$ *in* (3.2) *must be understood as a term independent of* λ^{P} *since, from the definitions introduced in section* 2 *for* $\boldsymbol{f}^{\mathrm{P}}$ *and* $\boldsymbol{f}^{\mathrm{E}}$*, and asuming that* $(\mu^{\mathrm{P}} + \lambda^{\mathrm{P}}) \sim (\mu^{\mathrm{E}} + \lambda^{\mathrm{E}})$*, we deduce that* $(\mu^{\mathrm{P}} + \lambda^{\mathrm{P}})(\|\boldsymbol{f}^{\mathrm{P}}\|_{0,\Omega^{\mathrm{P}}} + \|\boldsymbol{f}^{\mathrm{E}}\|_{0,\Omega^{\mathrm{E}}}) \sim (\|\widetilde{\boldsymbol{f}}^{\mathrm{P}}\|_{0,\Omega^{\mathrm{P}}} + \|\widetilde{\boldsymbol{f}}^{\mathrm{E}}\|_{0,\Omega^{\mathrm{E}}})$.

Remark 3.2. *In the case that* $c_0 \to 0$ *in* (2.2)*, the problem for the fluid pressure* p^{P} *defined in* (2.1)-(2.2) *is not well-posed in* $\mathrm{H}^1(\Omega^{\mathrm{P}})$*. However, uniqueness is restored by asking the solution to live in* $\mathrm{H}^1(\Omega^{\mathrm{P}}) \cap \mathrm{L}^2_0(\Omega^{\mathrm{P}})$*, where* $\mathrm{L}^2_0(\Omega^{\mathrm{P}}) := \{q \in \mathrm{L}^2(\Omega^{\mathrm{P}}) : \int_{\Omega^{\mathrm{P}}} q = 0\}$*. As this new space is a closed subspace of* $\mathrm{H}^1(\Omega^{\mathrm{P}})$ *where the norm and seminorm are equivalent, the stability analysis of* (2.17)-(2.19) *follows exactly as in Lemma* 3.2*, with the constant* c_1 *in* (3.6) *now defined as* $c_1 := c_p \kappa_1 \xi^{-1}$*, with* c_p *representing the Poincaré constant.*

3.2. Solvability of the continuous problem. We now address the unique solvability of (2.17)-(2.19) applying Fredholm's alternative theory for compact operators. Let us recast the system (2.17)-(2.19) as the following equivalent operator problem: find $\vec{\boldsymbol{u}} := (\vec{\boldsymbol{\omega}}, \boldsymbol{u}, p^{\mathrm{P}}) \in \mathbf{X} := \mathbf{H} \times \mathbf{V} \times \mathrm{Q}^{\mathrm{P}}$ such that

$$(\mathcal{S} + \mathcal{T})\vec{\boldsymbol{u}} = \mathcal{F}, \tag{3.9}$$

where the linear operators $\mathcal{S} : \mathbf{X} \to \mathbf{X}^{\star}$, $\mathcal{T} : \mathbf{X} \to \mathbf{X}^{\star}$, and $\mathcal{F} \in \mathbf{X}^{\star}$ are defined as

$$\begin{aligned} \langle \mathcal{S}(\vec{\boldsymbol{u}}), \vec{\boldsymbol{v}} \rangle &: = a(\vec{\boldsymbol{\omega}}, \vec{\boldsymbol{\theta}}) + b_1(\vec{\boldsymbol{\theta}}, \boldsymbol{u}) - b_1(\vec{\boldsymbol{\omega}}, \boldsymbol{v}) + c(p^{\mathrm{P}}, q^{\mathrm{P}}), \\ \langle \mathcal{T}(\vec{\boldsymbol{u}}), \vec{\boldsymbol{v}} \rangle &: = -b_2(\vec{\boldsymbol{\theta}}, p^{\mathrm{P}}) - b_3(\vec{\boldsymbol{\omega}}, q^{\mathrm{P}}), \\ \langle \mathcal{F}, \vec{\boldsymbol{v}} \rangle &: = -F(\boldsymbol{v}) - G(q^{\mathrm{P}}), \end{aligned}$$

for all $\vec{\boldsymbol{u}} := (\vec{\boldsymbol{\omega}}, \boldsymbol{u}, p^{\mathrm{P}})$, $\vec{\boldsymbol{v}} := (\vec{\boldsymbol{\theta}}, \boldsymbol{v}, q^{\mathrm{P}}) \in \mathbf{X}$, where we recall that $\langle \cdot, \cdot \rangle$ stands for the duality pairing between the space $\mathbf{X}$ and its dual $\mathbf{X}^{\star}$.

The three upcoming lemmas establish the invertibility of $\mathcal{S}$, the compactness of $\mathcal{T}$, and the injectivity of $\mathcal{S} + \mathcal{T}$, such that Fredholm's theory implies the well-posedness of the operator problem (3.9), and equivalently of (2.17)-(2.19).

Lemma 3.3. *The operator* $\mathcal{S} : \mathbf{X} \to \mathbf{X}^{\star}$ *is invertible.*

Proof. First, for a given functional $\mathcal{F} := (\mathcal{F}_{\mathbf{H}}, \mathcal{F}_{\mathbf{V}}, \mathcal{F}_{\mathrm{Q}^{\mathrm{P}}})$, observe that establishing the invertibility of $\mathcal{S}$ is equivalent to proving the unique solvability of the operator problem

$$\mathcal{S}(\vec{\boldsymbol{u}}) = \mathcal{F}. \tag{3.10}$$

Furthermore, proving unique solvability of (3.10) is in turn equivalent to proving the unique solvability of the two following uncoupled problems: find $(\vec{\boldsymbol{\omega}}, \boldsymbol{u}) \in \mathbf{H} \times \mathbf{V}$ such that

$$\begin{aligned} a(\vec{\boldsymbol{\omega}}, \vec{\boldsymbol{\theta}}) + b_1(\vec{\boldsymbol{\theta}}, \boldsymbol{u}) &= F_{\mathbf{H}}(\vec{\boldsymbol{\theta}}) \qquad \forall \vec{\boldsymbol{\theta}} \in \mathbf{H}, \\ b_1(\vec{\boldsymbol{\omega}}, \boldsymbol{v}) &= F_{\mathbf{V}}(\boldsymbol{v}) \qquad \forall \boldsymbol{v} \in \mathbf{V}, \end{aligned} \tag{3.11}$$

and: find $p^{\mathrm{P}} \in \mathrm{Q}^{\mathrm{P}}$, such that

$$c(p^{\mathrm{P}}, q^{\mathrm{P}}) = F_{\mathrm{Q}^{\mathrm{P}}}(q^{\mathrm{P}}) \qquad \forall q^{\mathrm{P}} \in \mathrm{Q}^{\mathrm{P}}, \tag{3.12}$$

where $F_{\mathbf{H}}$, $F_{\mathbf{V}}$, and $F_{\mathrm{Q^P}}$ are the functionals induced by $\mathcal{F}_{\mathbf{H}}$, $\mathcal{F}_{\mathbf{V}}$, and $\mathcal{F}_{\mathrm{Q^P}}$, respectively.

Observe that the unique solvability of the latter problem (3.12) follows by virtue of the well-known Lax-Milgram lemma. In turn, according to the continuity of $a(\cdot,\cdot)$ and $b_1(\cdot,\cdot)$, the ellipticity of $a(\cdot,\cdot)$ and the inf-sup condition of $b_1(\cdot,\cdot)$, the well-posedness of (3.11) follows from a straightforward application of the Babuška-Brezzi theory (see, e.g. [10, Theorem 2.3]), completing the proof. ∎

Lemma 3.4. *The operator $\mathcal{T}:\mathbf{X}\to\mathbf{X}^\star$ is compact.*

Proof. We begin by defining the operator $\mathbb{B}:\mathrm{L}^2(\Omega^{\mathrm{P}})\to\mathrm{Q}^{\mathrm{P}}$ as

$$\langle\mathbb{B}(\psi^{\mathrm{P}}),q^{\mathrm{P}}\rangle_{0,\Omega^{\mathrm{P}}} := \alpha(1+\eta^{\mathrm{P}})^{-1}\int_{\Omega^{\mathrm{P}}} q^{\mathrm{P}}\psi^{\mathrm{P}} \qquad \forall\, q^{\mathrm{P}}\in\mathrm{Q}^{\mathrm{P}},\forall\,\psi^{\mathrm{P}}\in\mathrm{L}^2(\Omega^{\mathrm{P}}),$$

where $\langle\cdot,\cdot\rangle_{0,\Omega^{\mathrm{P}}}$ denotes the $\mathrm{L}^2(\Omega^{\mathrm{P}})$-inner product. This operator is compact since it is constituted by the composition of a compact injection and a continuous map (see, [22, Lemma 2.2] for further details). Thus, denoting by $\mathbb{B}^\star$ the adjoint of $\mathbb{B}$, we infer that the operator

$$\mathcal{T}(\vec{\boldsymbol{u}}) = ((\mathbf{0},-(\mu^{\mathrm{P}}+\lambda^{\mathrm{P}})^{-1}\mathbb{B}(\phi^{\mathrm{P}}),\mathbf{0},0),\mathbf{0},-\mathbb{B}^\star(p^{\mathrm{P}})),$$

is also compact. ∎

Lemma 3.5. *The operator $(\mathcal{S}+\mathcal{T}):\mathbf{X}\to\mathbf{X}^\star$ is injective.*

Proof. By definition of the linear operator $(\mathcal{S}+\mathcal{T}):\mathbf{X}\to\mathbf{X}^\star$, observe that it is sufficient to show that the only solution to the homogeneous problem

$$\begin{aligned} a(\vec{\boldsymbol{\omega}},\vec{\boldsymbol{\theta}})+b_1(\vec{\boldsymbol{\theta}},\boldsymbol{u})-b_2(\vec{\boldsymbol{\theta}},p^{\mathrm{P}}) &= 0 \qquad \forall\,\vec{\boldsymbol{\theta}}\in\mathbf{H},\\ b_1(\vec{\boldsymbol{\omega}},\boldsymbol{v}) &= 0 \qquad \forall\,\boldsymbol{v}\in\mathbf{V},\\ b_3(\vec{\boldsymbol{\omega}},q^{\mathrm{P}})-c(p^{\mathrm{P}},q^{\mathrm{P}}) &= 0 \qquad \forall\,q^{\mathrm{P}}\in\mathrm{Q}^{\mathrm{P}}, \end{aligned}$$

is the null-vector in the product space $\mathbf{X}$. Thus, from (3.6), (3.7), and the fact that $F=G=0$, we deduce that $\vec{\boldsymbol{\omega}}=\mathbf{0}$ and $p=0$. Then, with this in mind, we apply (3.8) and obtain $\boldsymbol{u}=\mathbf{0}$, which finishes the proof. ∎

By virtue of Lemmas 3.2, 3.3, 3.4, and 3.5, and the abstract Fredholm alternative theorem, one straightforwardly derives the main result of this section, stated in the upcoming theorem.

Theorem 3.1. *There exists a unique solution $(\vec{\boldsymbol{\omega}},\boldsymbol{u},p^{\mathrm{P}})\in\mathbf{H}\times\mathbf{V}\times\mathrm{Q}^{\mathrm{P}}$ to the coupled problem (2.17)-(2.19). Furthermore, there exists a positive constant $C>0$, independent of η^{P} and η^{E}, such that*

$$\|\vec{\boldsymbol{\omega}}\|_{\mathbf{H}}+\|\boldsymbol{u}\|_{\mathbf{V}}+\|p^{\mathrm{P}}\|_{1,\Omega^{\mathrm{P}}}\leq C\big\{(\mu^{\mathrm{P}}+\lambda^{\mathrm{P}})(\|\boldsymbol{f}^{\mathrm{E}}\|_{0,\Omega^{\mathrm{E}}}+\|\boldsymbol{f}^{\mathrm{P}}\|_{0,\Omega^{\mathrm{P}}})+\|\boldsymbol{g}\|_{0,\Omega^{\mathrm{P}}}+\|s^{\mathrm{P}}\|_{0,\Omega^{\mathrm{P}}}\big\}.$$

4. Finite element discretisation.

4.1. Discrete spaces and Galerkin formulation. Let $\{\mathcal{T}_h\}_{h>0}$ be a shape-regular family of partitions of the closed domain $\bar{\Omega}$, conformed by tetrahedra (or triangles in 2D) T of diameter h_T, with mesh size $h:=\max\{h_T:\ T\in\mathcal{T}_h\}$. Given an integer $k\geq 0$ and a subset S of $\mathbb{R}^d$, $d=2,3$, by $\mathbb{P}_k(S)$ we will denote the space of polynomial functions defined locally in S and being of total degree up to k.

We specify the finite-dimensional subspaces of the functional spaces for global displacement, fluid poroelastic pressure, poroelastic rotations, total poroelastic pressure, elastic rotations, and solid pressure; as follows

$$\mathbf{V}_h := \{\boldsymbol{v}_h\in\mathbf{C}(\overline{\Omega})\cap\mathbf{V}:\boldsymbol{v}_h|_T\in\mathbb{P}_{k+1}(T)^d,\ \forall T\in\mathcal{T}_h\},$$

$$
\begin{aligned}
\mathrm{Q}_h^{\mathrm{P}} &:= \{q_h^{\mathrm{P}} \in \mathrm{C}(\overline{\Omega^{\mathrm{P}}}) \cap \mathrm{Q}^{\mathrm{P}} : q_h^{\mathrm{P}}|_T \in \mathbb{P}_{k+1}(T),\ \forall T \in \mathcal{T}_h\},\\
\mathbf{W}_h^{\mathrm{P}} &:= \{\boldsymbol{\theta}_h^{\mathrm{P}} \in \mathbf{L}^2(\Omega^{\mathrm{P}}) : \boldsymbol{\theta}_h^{\mathrm{P}}|_T \in \mathbb{P}_k(T)^d,\ \forall T \in \mathcal{T}_h\},\\
\mathrm{Z}_h^{\mathrm{P}} &:= \{\psi_h^{\mathrm{P}} \in \mathrm{L}^2(\Omega^{\mathrm{P}}) : \psi_h^{\mathrm{P}}|_T \in \mathbb{P}_k(T),\ \forall T \in \mathcal{T}_h\},\\
\mathbf{W}_h^{\mathrm{E}} &:= \{\boldsymbol{\theta}_h^{\mathrm{E}} \in \mathbf{L}^2(\Omega^{\mathrm{E}}) : \boldsymbol{\theta}_h^{\mathrm{E}}|_T \in \mathbb{P}_k(T)^d,\ \forall T \in \mathcal{T}_h\},\\
\mathrm{Q}_h^{\mathrm{E}} &:= \{q_h^{\mathrm{E}} \in \mathrm{L}^2(\Omega^{\mathrm{E}}) : q_h^{\mathrm{E}}|_T \in \mathbb{P}_k(T),\ \forall T \in \mathcal{T}_h\}.
\end{aligned} \tag{4.1}
$$

In this way, denoting by $\vec{\boldsymbol{\omega}}_h := (\boldsymbol{\omega}_h^{\mathrm{P}}, \phi_h^{\mathrm{P}}, \boldsymbol{\omega}_h^{\mathrm{E}}, p_h^{\mathrm{E}}) \in \mathbf{W}_h^{\mathrm{P}} \times \mathrm{Z}_h^{\mathrm{P}} \times \mathbf{W}_h^{\mathrm{E}} \times \mathrm{Q}_h^{\mathrm{E}} := \mathbf{H}_h$, the proposed Galerkin finite element scheme approximating (2.17)-(2.19) reads as follows: find $(\vec{\boldsymbol{\omega}}_h, \boldsymbol{u}_h, p_h^{\mathrm{P}}) \in \mathbf{H}_h \times \mathbf{V}_h \times \mathrm{Q}_h^{\mathrm{P}}$ such that

$$
a(\vec{\boldsymbol{\omega}}_h, \vec{\boldsymbol{\theta}}_h) + b_1(\vec{\boldsymbol{\theta}}_h, \boldsymbol{u}_h) - b_2(\vec{\boldsymbol{\theta}}_h, p_h^{\mathrm{P}}) = 0 \qquad \forall\, \vec{\boldsymbol{\theta}}_h \in \mathbf{H}_h, \tag{4.2}
$$

$$
b_1(\vec{\boldsymbol{\omega}}_h, \boldsymbol{v}_h) = F(\boldsymbol{v}_h) \qquad \forall\, \boldsymbol{v}_h \in \mathbf{V}_h, \tag{4.3}
$$

$$
b_3(\vec{\boldsymbol{\omega}}_h, q_h^{\mathrm{P}}) - c(p_h^{\mathrm{P}}, q_h^{\mathrm{P}}) = G(q_h^{\mathrm{P}}) \qquad \forall\, q_h^{\mathrm{P}} \in \mathrm{Q}_h^{\mathrm{P}}, \tag{4.4}
$$

where $\vec{\boldsymbol{\theta}}_h := (\boldsymbol{\theta}_h^{\mathrm{P}}, \psi_h^{\mathrm{P}}, \boldsymbol{\theta}_h^{\mathrm{E}}, q_h^{\mathrm{E}})$.

4.2. Solvability and stability of the discrete problem. It is evident that all bilinear forms and functionals introduced in Section 2 preserve the relevant stability properties on the corresponding discrete spaces. Furthermore, it is clear that the bilinear forms $a(\cdot,\cdot)$, and $c(\cdot,\cdot)$ also maintain the coercivity on the discrete spaces $\mathbf{H}_h$ and $\mathrm{Q}_h^{\mathrm{P}}$, respectively. Moreover, we notice in advance that the continuous inf-sup condition (3.1) is also inherited at the discrete level for the particular choice of elements outlined in (4.1), and therefore, there exists a positive constant $\widehat{\beta}$ independent of h such that the following holds:

$$
\sup_{\vec{\boldsymbol{\theta}}_h \in \mathbf{H}_h \setminus \mathbf{0}} \frac{b_1(\vec{\boldsymbol{\theta}}_h, \boldsymbol{v}_h)}{\|\vec{\boldsymbol{\theta}}_h\|_{\mathbf{H}}} \geq \widehat{\beta} \|\boldsymbol{v}_h\|_{\mathbf{V}} \qquad \forall\, \boldsymbol{v}_h \in \mathbf{V}_h, \tag{4.5}
$$

where we once again mention that $\widehat{\beta}$ is independent of the auxiliary scaling parameters η^{P} and η^{E}.

Next, utilising the stability properties outlined above, we are ready to establish the well-posedness of the proposed Galerkin scheme (4.2)-(4.4).

Theorem 4.1. *There exists a unique solution $(\vec{\boldsymbol{\omega}}_h, \boldsymbol{u}_h, p_h^{\mathrm{P}}) \in \mathbf{H}_h \times \mathbf{V}_h \times \mathrm{Q}_h^{\mathrm{P}}$ to the discrete coupled problem (4.2)-(4.4). Furthermore, there exists a positive constant $C_{Stab} > 0$, independent of h, η^{P} and η^{E}, such that*

$$
\|\vec{\boldsymbol{\omega}}_h\|_{\mathbf{H}} + \|\boldsymbol{u}_h\|_{\mathbf{V}} + \|p_h^{\mathrm{P}}\|_{1,\Omega^{\mathrm{P}}} \leq C_{Stab}\big\{(\mu^{\mathrm{P}} + \lambda^{\mathrm{P}})(\|\boldsymbol{f}^{\mathrm{E}}\|_{0,\Omega^{\mathrm{E}}} + \|\boldsymbol{f}^{\mathrm{P}}\|_{0,\Omega^{\mathrm{P}}}) + \|\boldsymbol{g}\|_{0,\Omega^{\mathrm{P}}} + \|s^{\mathrm{P}}\|_{0,\Omega^{\mathrm{P}}}\big\}.
$$

Proof. First, for the stability analysis we proceed exactly as in the proof of Lemma 3.2. Thus, it is a laborious but straightforward exercise to verify that

$$
\begin{aligned}
c_1\|p_h^{\mathrm{P}}\|_{1,\Omega^{\mathrm{P}}}^2 &\leq (\mu^{\mathrm{P}} + \lambda^{\mathrm{P}})(\|\boldsymbol{f}^{\mathrm{P}}\|_{0,\Omega^{\mathrm{P}}} + \|\boldsymbol{f}^{\mathrm{E}}\|_{0,\Omega^{\mathrm{E}}})\|\boldsymbol{u}_h\|_{1,\Omega^{\mathrm{P}}} + (\rho\xi^{-1}\kappa_2\|\boldsymbol{g}\|_{0,\Omega^{\mathrm{P}}} + \|s^{\mathrm{P}}\|_{0,\Omega^{\mathrm{P}}})\|p_h^{\mathrm{P}}\|_{1,\Omega^{\mathrm{P}}},\\
\frac{1}{2(1+\eta^{\mathrm{P}})}\|\vec{\boldsymbol{\omega}}_h\|_{\mathbf{H}}^2 &\leq \frac{\alpha^2}{2(1+\eta^{\mathrm{P}})}\|p_h^{\mathrm{P}}\|_{0,\Omega^{\mathrm{P}}}^2 + 2(\|\boldsymbol{f}^{\mathrm{P}}\|_{0,\Omega^{\mathrm{P}}} + \|\boldsymbol{f}^{\mathrm{P}}\|_{0,\Omega^{\mathrm{E}}})\|\boldsymbol{u}_h\|_{1,\Omega^{\mathrm{P}}}\\
&\quad + (\rho\xi^{-1}\kappa_2\|\boldsymbol{g}\|_{0,\Omega^{\mathrm{P}}} + \|s^{\mathrm{P}}\|_{0,\Omega^{\mathrm{P}}})\|p_h^{\mathrm{P}}\|_{1,\Omega^{\mathrm{P}}},\\
\beta\|\boldsymbol{u}_h\|_{\mathbf{V}} &\leq \frac{\alpha}{(\mu^{\mathrm{P}} + \lambda^{\mathrm{P}})(1+\eta^{\mathrm{P}})}\|p_h^{\mathrm{P}}\| + \|\vec{\boldsymbol{\omega}}_h\|_{\mathbf{H}},
\end{aligned}
$$

which imply that there exists $C_{\mathrm{Stab}} > 0$, independent of h, η^{P} and η^{E}, such that

$$
\|\vec{\boldsymbol{\omega}}_h\|_{\mathbf{H}} + \|\boldsymbol{u}_h\|_{\mathbf{V}} + \|p_h^{\mathrm{P}}\|_{1,\Omega^{\mathrm{P}}} \leq C_{\mathrm{Stab}}\big\{(\mu^{\mathrm{P}} + \lambda^{\mathrm{P}})(\|\boldsymbol{f}^{\mathrm{E}}\|_{0,\Omega^{\mathrm{E}}} + \|\boldsymbol{f}^{\mathrm{P}}\|_{0,\Omega^{\mathrm{P}}}) + \|\boldsymbol{g}\|_{0,\Omega^{\mathrm{P}}} + \|s^{\mathrm{P}}\|_{0,\Omega^{\mathrm{P}}}\big\}. \tag{4.6}
$$

For the solvability analysis of the discrete scheme it is suffices to prove that the solution of the homogeneous problem is the trivial solution (since we are restricting to the finite dimensional case). For this purpose, we let $(\vec{\boldsymbol{\omega}}_h, \boldsymbol{u}_h, p_h^{\mathrm{P}}) \in \mathbf{H}_h \times \mathbf{V}_h \times \mathrm{Q}_h^{\mathrm{P}}$ the solution to the discrete coupled problem (4.2)-(4.4), where it is assumed that $\boldsymbol{f}^{\mathrm{E}} = \mathbf{0}$, $\boldsymbol{f}^{\mathrm{P}} = \mathbf{0}$, $\boldsymbol{g} = \mathbf{0}$ and $s^{\mathrm{P}} = 0$. Thus, proceeding as in the proof of Lemma 3.5, the result follows straightforwardly by (4.6). □

4.3. A priori error bounds. We are now in a position to derive the optimal a priori estimates for the Galerkin scheme (4.2)-(4.4). For this purpose, we first establish a Céa estimate formulated in the following theorem.

THEOREM 4.2. *Let $(\vec{\boldsymbol{\omega}}, \boldsymbol{u}, p^{\mathrm{P}})$ and $(\vec{\boldsymbol{\omega}}_h, \boldsymbol{u}_h, p_h^{\mathrm{P}})$ be the unique solutions of the continuous and discrete coupled problems (2.17)-(2.19) and (4.2)-(4.4), respectively. Then, there exists a strictly positive constant $C_{Céa} > 0$, independent of h, η^{P} and η^{E}, such that*

(4.7)
$$\|\vec{\boldsymbol{\omega}} - \vec{\boldsymbol{\omega}}_h\|_{\mathbf{H}} + \|\boldsymbol{u} - \boldsymbol{u}_h\|_{\mathbf{V}} + \|p^{\mathrm{P}} - p_h^{\mathrm{P}}\|_{1,\Omega^{\mathrm{P}}} \le C_{Céa}\big(\mathrm{dist}(\vec{\boldsymbol{\omega}}, \mathbf{H}_h) + \mathrm{dist}(\boldsymbol{u}, \mathbf{V}_h) + \mathrm{dist}(p^{\mathrm{P}}, \mathrm{Q}_h^{\mathrm{P}})\big).$$

Proof. First, we start by introducing the following discrete space:

$$\mathbf{K}_h := \{\vec{\boldsymbol{\theta}}_h \in \mathbf{H}_h : b_1(\vec{\boldsymbol{\theta}}_h, \boldsymbol{v}_h) = F(\boldsymbol{v}_h) \quad \forall \boldsymbol{v}_h \in \mathbf{V}_h\},$$

and observing, according to (4.3), that $\vec{\boldsymbol{\omega}}_h \in \mathbf{K}_h$ and that $(\vec{\boldsymbol{\omega}}_h - \vec{\boldsymbol{\chi}}_{\vec{\boldsymbol{\omega}},h}) \in \mathrm{Ker}_h(b_1) := \{\vec{\boldsymbol{\theta}}_h \in \mathbf{H}_h : b_1(\vec{\boldsymbol{\theta}}_h, \boldsymbol{v}_h) = 0 \quad \forall \boldsymbol{v}_h \in \mathbf{V}_h\} \quad \forall \vec{\boldsymbol{\chi}}_{\vec{\boldsymbol{\omega}},h} \in \mathbf{K}_h$. Moreover, following the arguments employed in [22, Theorem 3.2], we establish the corresponding Galerkin orthogonality property:

$$a(\vec{\boldsymbol{\omega}} - \vec{\boldsymbol{\omega}}_h, \vec{\boldsymbol{\theta}}_h) + b_1(\vec{\boldsymbol{\theta}}_h, \boldsymbol{u} - \boldsymbol{u}_h) - b_2(\vec{\boldsymbol{\theta}}_h, p^{\mathrm{P}} - p_h^{\mathrm{P}}) = 0 \qquad \forall \vec{\boldsymbol{\theta}}_h \in \mathbf{H}_h, \tag{4.8}$$
$$b_1(\vec{\boldsymbol{\omega}} - \vec{\boldsymbol{\omega}}_h, \boldsymbol{v}_h) = 0 \qquad \forall \boldsymbol{v}_h \in \mathbf{V}_h, \tag{4.9}$$
$$b_3(\vec{\boldsymbol{\omega}} - \vec{\boldsymbol{\omega}}_h, q_h^{\mathrm{P}}) - c(p^{\mathrm{P}} - p_h^{\mathrm{P}}, q_h^{\mathrm{P}}) = 0 \qquad \forall q_h^{\mathrm{P}} \in \mathrm{Q}_h^{\mathrm{P}}. \tag{4.10}$$

Thus, considering arbitrary $\boldsymbol{\chi}_{\boldsymbol{u},h} \in \mathbf{V}_h$ and $\chi_{p^{\mathrm{P}},h} \in \mathrm{Q}_h^{\mathrm{P}}$, we can deduce from (4.8) with $\vec{\boldsymbol{\theta}}_h = (\vec{\boldsymbol{\chi}}_{\vec{\boldsymbol{\omega}},h} - \vec{\boldsymbol{\omega}}_h) \in \mathrm{Ker}_h(b_1)$ that

$$\begin{aligned} a((\vec{\boldsymbol{\chi}}_{\vec{\boldsymbol{\omega}},h} - \vec{\boldsymbol{\omega}}_h), (\vec{\boldsymbol{\chi}}_{\vec{\boldsymbol{\omega}},h} - \vec{\boldsymbol{\omega}}_h)) &= -a((\vec{\boldsymbol{\omega}} - \vec{\boldsymbol{\chi}}_{\vec{\boldsymbol{\omega}},h}), (\vec{\boldsymbol{\chi}}_{\vec{\boldsymbol{\omega}},h} - \vec{\boldsymbol{\omega}}_h)) - b_1((\vec{\boldsymbol{\chi}}_{\vec{\boldsymbol{\omega}},h} - \vec{\boldsymbol{\omega}}_h), (\boldsymbol{u} - \boldsymbol{\chi}_{\boldsymbol{u},h})) \\ &\quad - b_1((\vec{\boldsymbol{\chi}}_{\vec{\boldsymbol{\omega}},h} - \vec{\boldsymbol{\omega}}_h), (\boldsymbol{\chi}_{\boldsymbol{u},h} - \boldsymbol{u}_h)) + b_2((\vec{\boldsymbol{\chi}}_{\vec{\boldsymbol{\omega}},h} - \vec{\boldsymbol{\omega}}_h), (p^{\mathrm{P}} - \chi_{p^{\mathrm{P}},h})) \\ &\quad + b_2((\vec{\boldsymbol{\chi}}_{\vec{\boldsymbol{\omega}},h} - \vec{\boldsymbol{\omega}}_h), (\chi_{p^{\mathrm{P}},h} - p_h^{\mathrm{P}})), \end{aligned}$$

which together with the ellipticity of $a(\cdot,\cdot)$ and the continuity of $a(\cdot,\cdot)$, $b_1(\cdot,\cdot)$ and $b_2(\cdot,\cdot)$, implies

(4.11)
$$\frac{\|\vec{\boldsymbol{\chi}}_{\vec{\boldsymbol{\omega}},h} - \vec{\boldsymbol{\omega}}_h\|_{\mathbf{H}}}{(1+\eta^{\mathrm{P}})} \le C_1\{\|\vec{\boldsymbol{\omega}} - \vec{\boldsymbol{\chi}}_{\vec{\boldsymbol{\omega}},h}\|_{\mathbf{H}} + \|\boldsymbol{u} - \boldsymbol{\chi}_{\boldsymbol{u},h}\|_{\mathbf{V}} + \|p^{\mathrm{P}} - \chi_{p^{\mathrm{P}},h}\|_{1,\Omega^{\mathrm{P}}}\} + \frac{\alpha\|\chi_{p^{\mathrm{P}},h} - p_h^{\mathrm{P}}\|_{0,\Omega^{\mathrm{P}}}}{(\mu^{\mathrm{P}}+\lambda^{\mathrm{P}})(1+\eta^{\mathrm{P}})},$$

with $C_1 > 0$, independent of h, η^{P} and η^{E}.

In turn, from (4.10) with $q_h^{\mathrm{P}} = \chi_{p^{\mathrm{P}},h} - p_h^{\mathrm{P}}$, we have

$$\begin{aligned} c((\chi_{p^{\mathrm{P}},h} - p_h^{\mathrm{P}}), (\chi_{p^{\mathrm{P}},h} - p_h^{\mathrm{P}})) &= -c((p^{\mathrm{P}} - \chi_{p^{\mathrm{P}},h}), (\chi_{p^{\mathrm{P}},h} - p_h^{\mathrm{P}})) - b_3((\vec{\boldsymbol{\chi}}_{\vec{\boldsymbol{\omega}},h} - \vec{\boldsymbol{\omega}}_h), (\chi_{p^{\mathrm{P}},h} - p_h^{\mathrm{P}})) \\ &\quad - b_3((\vec{\boldsymbol{\omega}} - \vec{\boldsymbol{\chi}}_{\vec{\boldsymbol{\omega}},h}), (\chi_{p^{\mathrm{P}},h} - p_h^{\mathrm{P}})). \end{aligned}$$

In this way, applying the ellipticity of $c(\cdot,\cdot)$ and the continuity of $c(\cdot,\cdot)$ and $b_3(\cdot,\cdot)$, we obtain

$$\left[c_0 + \frac{\alpha^2}{(\mu^{\mathrm{P}}+\lambda^{\mathrm{P}})(1+\eta^{\mathrm{P}})}\right]\|\chi_{p^{\mathrm{P}},h} - p_h^{\mathrm{P}}\|^2_{0,\Omega^{\mathrm{P}}} + \frac{\kappa_1}{\xi}|\chi_{p^{\mathrm{P}},h} - p_h^{\mathrm{P}}|^2_{1,\Omega^{\mathrm{P}}}$$

$$\leq C_2 \left\{ \|\vec{\boldsymbol{\omega}} - \vec{\boldsymbol{\chi}}_{\vec{\boldsymbol{\omega}},h}\|_{\mathbf{H}} + \|(p^{\mathrm{P}} - \chi_{p^{\mathrm{P}},h})\|_{1,\Omega^{\mathrm{P}}} \right\} \|\chi_{p^{\mathrm{P}},h} - p_h^{\mathrm{P}}\|_{1,\Omega^{\mathrm{P}}} + \frac{\alpha}{(1+\eta^{\mathrm{P}})} \|\vec{\boldsymbol{\chi}}_{\vec{\boldsymbol{\omega}},h} - \vec{\boldsymbol{\omega}}_h\|_{\mathbf{H}} \|\chi_{p^{\mathrm{P}},h} - p_h^{\mathrm{P}}\|_{0,\Omega^{\mathrm{P}}},$$

which together with (4.11) implies

$$\|\chi_{p^{\mathrm{P}},h} - p_h^{\mathrm{P}}\|_{1,\Omega^{\mathrm{P}}} \leq \frac{C_3}{c_1} \left\{ \|\vec{\boldsymbol{\omega}} - \vec{\boldsymbol{\chi}}_{\vec{\boldsymbol{\omega}},h}\|_{\mathbf{H}} + \|\boldsymbol{u} - \boldsymbol{\chi}_{\boldsymbol{u},h}\|_{\mathbf{V}} + \|p^{\mathrm{P}} - \chi_{p^{\mathrm{P}},h}\|_{1,\Omega^{\mathrm{P}}} \right\}, \tag{4.12}$$

with $C_3 > 0$, independent of h, η^{P} and η^{E}.

It is also important to notice that inequalities (4.11) and (4.12) imply that

$$\|p^{\mathrm{P}} - p_h^{\mathrm{P}}\|_{1,\Omega^{\mathrm{P}}} \leq \left(1 + \frac{C_3}{c_1}\right) \|p^{\mathrm{P}} - \chi_{p^{\mathrm{P}},h}\|_{1,\Omega^{\mathrm{P}}} + \frac{C_3}{c_1} \left\{ \|\vec{\boldsymbol{\omega}} - \vec{\boldsymbol{\chi}}_{\vec{\boldsymbol{\omega}},h}\|_{\mathbf{H}} + \|\boldsymbol{u} - \boldsymbol{\chi}_{\boldsymbol{u},h}\|_{\mathbf{V}} \right\},$$

$$\|\vec{\boldsymbol{\omega}} - \vec{\boldsymbol{\omega}}_h\|_{\mathbf{H}} \leq \left(1 + C_1 + \frac{\alpha C_3}{c_1(\mu^{\mathrm{P}} + \lambda^{\mathrm{P}})}\right) \left\{ \|\vec{\boldsymbol{\omega}} - \vec{\boldsymbol{\chi}}_{\vec{\boldsymbol{\omega}},h}\|_{\mathbf{H}} + \|\boldsymbol{u} - \boldsymbol{\chi}_{\boldsymbol{u},h}\|_{\mathbf{V}} + \|p^{\mathrm{P}} - \chi_{p^{\mathrm{P}},h}\|_{1,\Omega^{\mathrm{P}}} \right\}.$$

And next, by combining the discrete inf-sup condition (4.5), (4.8) and the continuity of $a(\cdot,\cdot)$, $b_1(\cdot,\cdot)$ and $b_2(\cdot,\cdot)$, one readily infers that there exists $C_4 > 0$, independent of h, η^{P} and η^{E}, such that

$$\begin{aligned} \|\boldsymbol{\chi}_{u,h} - \boldsymbol{u}_h\|_{\mathbf{V}} &\leq \widehat{\beta}^{-1} \sup_{\vec{\boldsymbol{\theta}}_h \in \mathbf{H}_h \setminus \mathbf{0}} \frac{|b_1(\vec{\boldsymbol{\theta}}_h, (\boldsymbol{\chi}_{u,h} - \boldsymbol{u}_h))|}{\|\vec{\boldsymbol{\theta}}_h\|_{\mathbf{H}}} \\ &= \widehat{\beta}^{-1} \sup_{\vec{\boldsymbol{\theta}}_h \in \mathbf{H}_h \setminus \mathbf{0}} \frac{|a((\vec{\boldsymbol{\omega}} - \vec{\boldsymbol{\omega}}_h), \vec{\boldsymbol{\theta}}_h) + b_1(\vec{\boldsymbol{\theta}}_h, (\boldsymbol{u} - \boldsymbol{\chi}_{u,h})) + b_2(\vec{\boldsymbol{\theta}}_h, (p^{\mathrm{P}} - p_h^{\mathrm{P}}))|}{\|\vec{\boldsymbol{\theta}}_h\|_{\mathbf{H}}} \\ &\leq C_4 \big(\|\vec{\boldsymbol{\omega}} - \vec{\boldsymbol{\omega}}_h\|_{\mathbf{H}} + \|\boldsymbol{u} - \boldsymbol{\chi}_{u,h}\|_{\mathbf{V}} + \|p^{\mathrm{P}} - p_h^{\mathrm{P}}\|_{1,\Omega^{\mathrm{P}}} \big). \end{aligned} \tag{4.13}$$

Finally, recalling from [10, Theorem 2.6] that

$$\mathrm{dist}(\vec{\boldsymbol{\omega}}, \mathbf{K}_h) \leq \widetilde{C} \mathrm{dist}(\vec{\boldsymbol{\omega}}, \mathbf{H}_h),$$

and the fact that $\vec{\boldsymbol{\chi}}_{\vec{\boldsymbol{\omega}},h}, \boldsymbol{\chi}_{\boldsymbol{u},h}$ and $\chi_{p^{\mathrm{P}},h}$ are arbitrary, the desired result follows simply by using the triangle inequality, and the estimates (4.11)-(4.13). □

Finally, approximation properties of the spaces in (4.1) can be found in e.g [4, 10], which combined with the Céa's estimate (4.7) produce the theoretical rate of convergence of (4.2)-(4.4), summarised in what follows.

THEOREM 4.3. *In addition to the hypotheses of Theorems 3.1, 4.1 and 4.2, assume that there exists $s > 0$ such that $\boldsymbol{\omega}^{\mathrm{P}} \in \mathbf{H}^s(\Omega^{\mathrm{P}})$, $\boldsymbol{u} \in \mathbf{H}^{1+s}(\Omega)$, $\phi^{\mathrm{P}} \in \mathrm{H}^s(\Omega^{\mathrm{P}})$, $p^{\mathrm{P}} \in \mathrm{H}^{1+s}(\Omega^{\mathrm{P}})$, $\boldsymbol{\omega}^{\mathrm{E}} \in \mathbf{H}^s(\Omega^{\mathrm{E}})$ and $p^{\mathrm{E}} \in \mathrm{H}^s(\Omega^{\mathrm{E}})$. Then, there exist positive constant $C_{Conv} > 0$, independent of h, η^{P} and η^{E} such that with the finite element subspaces defined by (4.1), there holds*

$$\|\vec{\boldsymbol{\omega}} - \vec{\boldsymbol{\omega}}_h\|_{\mathbf{H}} + \|\boldsymbol{u} - \boldsymbol{u}_h\|_{\mathbf{V}} + \|p^{\mathrm{P}} - p_h^{\mathrm{P}}\|_{1,\Omega^{\mathrm{P}}} \leq C_{Conv}\, h^{\min\{s,k+1\}} \big(\|\boldsymbol{\omega}^{\mathrm{P}}\|_{s,\Omega^{\mathrm{P}}} + \|\boldsymbol{u}\|_{s+1,\Omega} + \|\phi^{\mathrm{P}}\|_{s,\Omega^{\mathrm{P}}} + \|p^{\mathrm{P}}\|_{s+1,\Omega^{\mathrm{P}}} + \|\boldsymbol{\omega}^{\mathrm{E}}\|_{s,\Omega^{\mathrm{E}}} + \|p^{\mathrm{E}}\|_{s,\Omega^{\mathrm{E}}} \big).$$

4.4. Suggested block structure. To close this section we proceed to rewrite the system (4.2)-(4.4) in a double saddle-point structure. For this purpose, we introduce the operators and functionals $\mathcal{A}^{\mathrm{P}} : \mathbf{W}_h^{\mathrm{P}} \times \mathrm{Z}_h^{\mathrm{P}} \to (\mathbf{W}_h^{\mathrm{P}} \times \mathrm{Z}_h^{\mathrm{P}})'$, $\mathcal{B}_1^{\mathrm{P}} : \mathbf{W}_h^{\mathrm{P}} \times \mathrm{Z}_h^{\mathrm{P}} \to (\mathbf{V}_h)'$, $\mathcal{B}_2^{\mathrm{P}} : \mathrm{Q}_h^{\mathrm{P}} \to (\mathbf{W}_h^{\mathrm{P}} \times \mathrm{Z}_h^{\mathrm{P}})'$, $\mathcal{B}_3^{\mathrm{P}} : \mathbf{W}_h^{\mathrm{P}} \times \mathrm{Z}_h^{\mathrm{P}} \to (\mathrm{Q}_h^{\mathrm{P}})'$, $\mathcal{A}^{\mathrm{E}} : \mathbf{W}_h^{\mathrm{E}} \times \mathrm{Q}_h^{\mathrm{E}} \to (\mathbf{W}_h^{\mathrm{E}} \times \mathrm{Q}_h^{\mathrm{E}})'$, $\mathcal{B}_1^{\mathrm{E}} : \mathbf{W}_h^{\mathrm{E}} \times \mathrm{Q}_h^{\mathrm{E}} \to (\mathbf{V}_h)'$, $\mathcal{C} : \mathrm{Q}_h^{\mathrm{P}} \to (\mathrm{Q}_h^{\mathrm{P}})'$, $\mathcal{F}^{\mathrm{P}}$, $\mathcal{F}^{\mathrm{E}} \in (\mathbf{V}_h)'$, $\mathcal{G} \in (\mathrm{Q}_h^{\mathrm{P}})'$, which are specified as

$$[\mathcal{A}^{\mathrm{P}}(\boldsymbol{\omega}_h^{\mathrm{P}}, \phi_h^{\mathrm{P}}), (\boldsymbol{\theta}_h^{\mathrm{P}}, \psi_h^{\mathrm{P}})] := \int_{\Omega^{\mathrm{P}}} \boldsymbol{\omega}_h^{\mathrm{P}} \cdot \boldsymbol{\theta}_h^{\mathrm{P}} + \frac{1}{1+\eta^{\mathrm{P}}} \int_{\Omega^{\mathrm{P}}} \phi_h^{\mathrm{P}} \psi_h^{\mathrm{P}},$$

$$
\begin{aligned}
[\mathcal{A}^{\mathrm{E}}(\boldsymbol{\omega}_h^{\mathrm{E}},p_h^{\mathrm{E}}),(\boldsymbol{\theta}_h^{\mathrm{E}},q_h^{\mathrm{E}})] &:= \int_{\Omega^{\mathrm{E}}} \boldsymbol{\omega}_h^{\mathrm{E}}\cdot\boldsymbol{\theta}_h^{\mathrm{E}} + \int_{\Omega^{\mathrm{E}}} p_h^{\mathrm{E}} q_h^{\mathrm{E}},\\
[\mathcal{B}_1^{\mathrm{P}}(\boldsymbol{\theta}_h^{\mathrm{P}},\psi_h^{\mathrm{P}}),\boldsymbol{v}_h] &:= -\sqrt{\eta^{\mathrm{P}}}\int_{\Omega^{\mathrm{P}}} \boldsymbol{\theta}_h^{\mathrm{P}}\cdot\mathbf{curl}\,\boldsymbol{v}_h + \int_{\Omega^{\mathrm{P}}}\psi_h^{\mathrm{P}}\operatorname{div}\boldsymbol{v}_h,\\
[\mathcal{B}_1^{\mathrm{E}}(\boldsymbol{\theta}_h^{\mathrm{E}},q_h^{\mathrm{E}}),\boldsymbol{v}_h] &:= -\sqrt{\eta^{\mathrm{E}}}\int_{\Omega^{\mathrm{E}}} \boldsymbol{\theta}_h^{\mathrm{E}}\cdot\mathbf{curl}\,\boldsymbol{v}_h + \int_{\Omega^{\mathrm{E}}} q_h^{\mathrm{E}}\operatorname{div}\boldsymbol{v}_h,
\end{aligned}
$$

$$
[\mathcal{B}_2^{\mathrm{P}}(\boldsymbol{\theta}_h^{\mathrm{P}},\psi_h^{\mathrm{P}}),p_h^{\mathrm{P}}] := \frac{\alpha}{(1+\eta^{\mathrm{P}})(\lambda^{\mathrm{P}}+\mu^{\mathrm{P}})}\int_{\Omega^{\mathrm{P}}} p_h^{\mathrm{P}}\psi_h^{\mathrm{P}},\quad [\mathcal{B}_3^{\mathrm{P}}(\boldsymbol{\omega}_h^{\mathrm{P}},\phi_h^{\mathrm{P}}),q_h^{\mathrm{P}}] := \frac{\alpha}{(1+\eta^{\mathrm{P}})}\int_{\Omega^{\mathrm{P}}} q_h^{\mathrm{P}}\phi_h^{\mathrm{P}},
$$

$$
\begin{aligned}
[\mathcal{C}(p_h^{\mathrm{P}}),q_h^{\mathrm{P}}] &:= \left[c_0 + \frac{\alpha^2}{(\mu^{\mathrm{P}}+\lambda^{\mathrm{P}})(1+\eta^{\mathrm{P}})}\right]\int_{\Omega^{\mathrm{P}}} p_h^{\mathrm{P}} q_h^{\mathrm{P}} + \frac{1}{\xi}\int_{\Omega^{\mathrm{P}}}\kappa\nabla p_h^{\mathrm{P}}\cdot\nabla q_h^{\mathrm{P}},\\
[\mathcal{F}^{\mathrm{P}},(\boldsymbol{v}_h)] &:= -\int_{\Omega^{\mathrm{P}}} \boldsymbol{f}^{\mathrm{P}}\cdot\boldsymbol{v}_h,\quad [\mathcal{F}^{\mathrm{E}},(\boldsymbol{v}_h)] := -\int_{\Omega^{\mathrm{E}}} \boldsymbol{f}^{\mathrm{E}}\cdot\boldsymbol{v}_h,\\
[\mathcal{G},(q_h^{\mathrm{P}})] &:= -\frac{\rho}{\xi}\int_{\Omega^{\mathrm{P}}}\kappa\boldsymbol{g}\cdot\nabla q_h^{\mathrm{P}} - \int_{\Omega^{\mathrm{P}}} s q_h^{\mathrm{P}},
\end{aligned}
$$

and arrive at the following double saddle point Galerkin scheme

$$
\begin{bmatrix}
\mathcal{A}^{\mathrm{P}} & 0 & (\mathcal{B}_1^{\mathrm{P}})' & -\mathcal{B}_2^{\mathrm{P}}\\
0 & \mathcal{A}^{\mathrm{E}} & (\mathcal{B}_1^{\mathrm{E}})' & \mathbf{0}\\
\mathcal{B}_1^{\mathrm{P}} & \mathcal{B}_1^{\mathrm{E}} & \mathbf{0} & \mathbf{0}\\
\mathcal{B}_3^{\mathrm{P}} & \mathbf{0} & \mathbf{0} & -\mathcal{C}
\end{bmatrix}
\begin{bmatrix}
(\boldsymbol{\omega}_h^{\mathrm{P}},\phi_h^{\mathrm{P}})\\
(\boldsymbol{\omega}_h^{\mathrm{E}},p_h^{\mathrm{E}})\\
\boldsymbol{u}_h\\
p_h^{\mathrm{P}}
\end{bmatrix}
=
\begin{bmatrix}
\mathbf{0}\\
\mathbf{0}\\
\mathcal{F}^{\mathrm{P}}+\mathcal{F}^{\mathrm{E}}\\
\mathcal{G}
\end{bmatrix}, \tag{4.14}
$$

which is precisely the way that the implementation is carried out. From this system it is clear that the coupling occurs only through the global displacement blocks. Notice also that (4.14) could be analysed using Fredholm's alternative theory in combination with an extension of the Babuška-Brezzi theory for multiple saddle-point problems [11, 19].

5. Computational examples. In this section we address the numerical verification of the convergence properties of the proposed schemes as well as the usability of these methods in a problem of more applicative interest. The solution of all linear systems in the form (4.14) and reported in this section, has been conducted with the Krylov method Flexible GMRES preconditioned with additive Schwarz using incomplete LU decomposition as local preconditioner.

Test 1: convergence verification. First we construct a sequence of successively refined uniform partitions of the elastic domain $\Omega = (0,1)^2$. The poroelastic region is $\Omega^{\mathrm{P}} = (0.25, 0.75)^2$ and the geometric setup is exemplified (for a coarse mesh) in the top-left panel of Figure 2. A closed-form solution for the global displacement satisfying (2.11) is as follows

$$
\boldsymbol{u}(x,y) = u_{\max}\begin{pmatrix} x(1-x)\cos(\pi x)\sin(2\pi y)\\ \sin(\pi x)\cos(\pi y)y^2(1-y)\end{pmatrix},
$$

where we use $u_{\max} = 0.1$. A material interface is considered between the two regions and so we impose a jump in the Young modulus and Poisson ratios of the solids $E^{\mathrm{P}} = 100$, $E^{\mathrm{E}} = 10000$, $\nu^{\mathrm{P}} = 0.3$, $\nu^{\mathrm{E}} = 0.45$. Consequently the exact rotations will have a different scaling in each domain. The remaining closed-form solutions and model constants are taken as follows

$$
\begin{gathered}
p^{\mathrm{E}} = -\operatorname{div}\boldsymbol{u},\quad p^{\mathrm{P}}(x,y) = \sin(\pi x)\sin(\pi y),\quad \phi^{\mathrm{P}} = \alpha(\lambda^{\mathrm{P}}+\mu^{\mathrm{P}})^{-1}p^{\mathrm{P}} - (1+\eta^{\mathrm{P}})\operatorname{div}\boldsymbol{u},\\
\boldsymbol{g} = \mathbf{0},\quad \kappa = 10^{-6},\quad \alpha = 0.1,\quad \xi = 10^{-2},\quad c_0 = 10^{-3}.
\end{gathered}
$$

The source terms (and for this example, also the remainders of the exact fluxes and traction forces on the interface) are imposed using these exact solutions. In Table 1 we collect the computed errors on each refinement level, separating each individual contribution to the errors in $\mathbf{H}$, that is, we show

$$
e(\boldsymbol{\omega}^{\mathrm{P}}) := \|\boldsymbol{\omega}^{\mathrm{P}} - \boldsymbol{\omega}_h^{\mathrm{P}}\|_{0,\Omega^{\mathrm{P}}},\quad e(\phi^{\mathrm{P}}) := \|\phi^{\mathrm{P}} - \phi_h^{\mathrm{P}}\|_{0,\Omega^{\mathrm{P}}},\quad e(\boldsymbol{\omega}^{\mathrm{E}}) := \|\boldsymbol{\omega}^{\mathrm{E}} - \boldsymbol{\omega}_h^{\mathrm{E}}\|_{0,\Omega^{\mathrm{E}}},
$$

h	$e(\boldsymbol{\omega}^{\mathrm{P}})$	rate	$e(\phi^{\mathrm{P}})$	rate	$e(\boldsymbol{\omega}^{\mathrm{E}})$	rate	$e(p^{\mathrm{E}})$	rate	$e(\boldsymbol{u})$	rate	$e(p^{\mathrm{P}})$	rate
$k=0$												
0.195	4.44e-3	–	8.73e-3	–	4.53e-3	–	1.27e-2	–	1.55e-2	–	2.34e-1	–
0.175	3.03e-3	2.531	4.85e-3	2.430	4.33e-3	0.428	1.16e-3	0.831	1.32e-2	1.470	1.16e-1	1.520
0.089	1.84e-3	0.838	2.90e-3	0.754	2.17e-3	1.020	6.02e-3	0.971	6.97e-3	0.945	6.48e-2	0.853
0.047	9.75e-4	0.889	1.63e-3	0.905	1.11e-3	1.051	3.02e-3	1.091	3.56e-3	1.061	3.49e-2	0.973
0.024	5.29e-4	0.998	8.28e-4	0.988	5.62e-4	0.992	1.54e-3	0.973	1.83e-3	0.972	1.84e-2	0.985
0.012	2.31e-4	1.170	5.41e-4	0.602	2.82e-4	0.997	7.54e-4	1.016	9.22e-4	0.963	9.59e-3	0.915
0.006	1.30e-5	0.835	2.47e-4	1.130	1.39e-4	1.034	3.73e-4	1.023	4.54e-4	1.030	4.92e-3	0.968
$k=1$												
0.195	8.51e-4	–	1.39e-3	–	8.36e-4	–	1.56e-3	–	2.24e-2	–	1.98e-1	–
0.175	2.40e-4	2.721	3.61e-4	2.402	6.06e-4	2.972	1.10e-3	3.225	1.31e-3	2.835	3.76e-2	2.504
0.089	7.58e-5	1.750	1.22e-4	1.692	1.55e-4	2.013	2.80e-4	2.014	3.40e-4	1.987	1.06e-2	1.686
0.047	2.57e-5	1.812	4.16e-5	1.769	4.13e-5	2.086	7.63e-5	2.040	9.53e-5	2.005	3.41e-3	1.759
0.024	7.52e-6	1.880	1.15e-5	1.987	1.01e-5	2.053	1.96e-5	1.981	2.47e-5	1.963	1.03e-4	1.798
0.012	1.88e-6	1.951	3.40e-6	1.972	2.50e-6	1.971	4.85e-6	1.973	6.26e-6	1.948	2.68e-5	1.896
0.006	4.81e-7	1.964	8.57e-7	1.983	6.07e-7	2.016	1.22e-6	1.998	1.52e-6	1.975	7.76e-6	1.952

Table 1

Test 1. Error history demonstrating the convergence predicted by Theorem 4.3, here illustrated for first- and second-order schemes.

$$e(p^{\mathrm{E}}) := \|p^{\mathrm{E}} - p_h^{\mathrm{E}}\|_{0,\Omega^{\mathrm{E}}}, \quad e(\boldsymbol{u}) := \|\boldsymbol{u} - \boldsymbol{u}_h\|_{\mathbf{V}}, \quad e(p^{\mathrm{P}}) := \|p^{\mathrm{P}} - p_h^{\mathrm{P}}\|_{1,\Omega^{\mathrm{P}}},$$

as well as the corresponding decay trend, $\texttt{rate} = \log\big(e(\cdot)/\widehat{e}(\cdot)\big)[\log(h/\widehat{h})]^{-1}$, where $e, \widehat{e}$ stand for errors generated on meshes with mesh sizes h and $\widehat{h}$, respectively. The tabulated results produced using the finite element spaces specified in (4.1) for $k=0$ and $k=1$ demonstrate numerically the optimal convergence order anticipated by Theorem 4.3.

Test 2: validation using augmented Mandel's problem. Secondly we conduct a benchmark test for poromechanics. We solve the classical Mandel problem, here extended to the case of coupled elastic-poroelastic structures following the configuration and parameter values from [16, 26]. The values of the constants are taken to be

$$c_0 = 2.5\text{e-}12\,\mathrm{Pa}^{-1}, \quad \alpha = 1, \quad \xi = 10^{-3}\mathrm{m}^2/s, \quad \mu^{\mathrm{E}} = \mu^{\mathrm{P}} = 10^8\,\mathrm{Pa}, \quad \nu^{\mathrm{E}} = \nu^{\mathrm{P}} = 0.2,$$
$$\kappa = 10^{-13}\,\mathrm{m}^2, \quad \rho = 1\,\mathrm{Kg/m}^3, \quad \widetilde{\boldsymbol{t}} = (0, -10^7)^{\mathtt{t}}\,\mathrm{Pa}\cdot\mathrm{m}.$$

For this problem the goal is to observe the so-called Mandel-Creyer effect, where the fluid pressure increases with time and then decreases over the poroelastic region. The elastic domain $\Omega^{\mathrm{E}} = (0,100)\times(20,40)\,\mathrm{m}^2$ is located on top of the poroelastic region $\Omega^{\mathrm{P}} = (0,100)\times(0,20)\,\mathrm{m}^2$, as shown in the schematic description of Figure 3 (left). The boundary conditions adopted for this test differ from (2.11). On the top of the elastic domain Γ^{top} we prescribe a constant traction $\widetilde{\boldsymbol{t}}$, on the right end of the elastic domain we set zero traction, and on the left of the elastic and poroelastic domains and on the bottom of the poroelastic domain we enforce a zero normal displacement; and on the right of the poroelastic domain we put $p^{\mathrm{P}} = 0$, whereas we impose $\kappa\nabla p^{\mathrm{P}}\cdot n = 0$ on the left and bottom of the poroelastic domain. We do not include gravitational effects for this test. Note that traction boundary conditions can be incorporated in the context of rotation-based formulations, by means of the additional term

$$[\mathcal{A}^{\boldsymbol{u}}(\boldsymbol{u}_h), \boldsymbol{v}_h] = \langle 2\eta^{\mathrm{E}}\nabla\boldsymbol{u}_h\boldsymbol{n}, \boldsymbol{v}_h\rangle_{\Gamma^{\mathrm{top}}\cup\Gamma^{\mathrm{E}}_{\mathrm{right}}} + \langle 2\,\mathrm{div}\,\boldsymbol{u}_h\boldsymbol{n}, \boldsymbol{v}_h\rangle_{\Gamma^{\mathrm{top}}\cup\Gamma^{\mathrm{E}}_{\mathrm{right}}}, \tag{5.1}$$

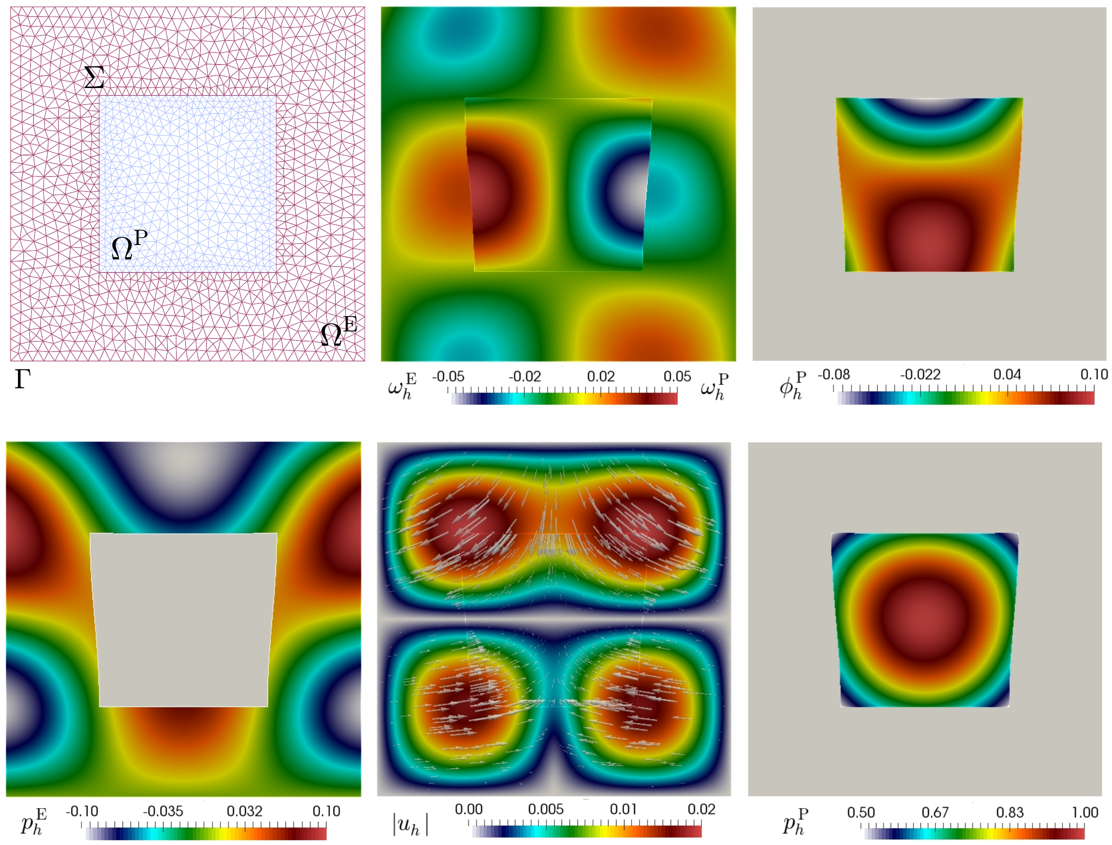

FIG. 2. *Test 1. Sketched mesh and domains before deformation (top left) and approximate solutions generated with a second-order scheme and plotted on the deformed configuration: rotations on each domain, total poroelastic pressure, elastic pressure, global displacement, and poroelastic fluid pressure.*

for the 2D case, or

$$[\mathcal{A}^{\boldsymbol{u}}(\boldsymbol{u}_h),\boldsymbol{v}_h] = -\langle 2\eta^{\rm E}\nabla\boldsymbol{u}_h\boldsymbol{n},\boldsymbol{v}_h\rangle_{\Gamma^{\rm top}\cup\Gamma^{\rm E}_{\rm right}} + \langle 2\eta^{\rm E}\,{\rm div}\,\boldsymbol{u}_h\boldsymbol{n},\boldsymbol{v}_h\rangle_{\Gamma^{\rm top}\cup\Gamma^{\rm E}_{\rm right}}, \tag{5.2}$$

in 3D, as part of the corresponding displacement block in (4.14) (see further details in [2, Sect. 3.2]), and adding the term

$$\langle\boldsymbol{t},\boldsymbol{v}_h\rangle_{\Gamma^{\rm top}\cup\Gamma^{\rm E}_{\rm right}} \quad \text{or} \quad -\langle\boldsymbol{t},\boldsymbol{v}_h\rangle_{\Gamma^{\rm top}\cup\Gamma^{\rm E}_{\rm right}},$$

in 2D or 3D, respectively, into $\mathcal{F}^{\rm E}$, appearing on the right-hand side of (4.14), with $\boldsymbol{t} := \widetilde{\boldsymbol{t}}/(\mu^{\rm E}+\lambda^{\rm E})$. Similar terms can be derived to impose traction conditions for the rotation-based formulation of the poroelasticity equation (2.13). Moreover, for simplicity when imposing traction conditions, in the present example we have used in both the elastic and poroelastic domains the same scaling $\eta^{\rm E}=\eta^{\rm P}$, and consequently on the right-hand sides we have the rescaling $1/(\mu^{\rm E}+\lambda^{\rm E}) = 1/(\mu^{\rm P}+\lambda^{\rm P})$. We use a structured triangular mesh and a first-order numerical scheme (setting $k=0$ in the finite element spaces (4.1)). We also incorporate time-dependence in the mass conservation equation (2.7), in the first two terms of the left-hand side, with initial conditions given by $p^{\rm P}(0)=0$ and $\phi^{\rm P}(0)=0$. We discretise in time with a backward Euler scheme, using a fixed time step $\Delta t = 1000\,$s and run the simulation for 5000 steps. We record fluid pressure profiles as well as horizontal displacements at different time instants and collect the results in the plots of Figure 3 (bottom panels). Even if the value of the maximal horizontal displacement is lower than that reported in [16, 26] (which can be explained by the differences in transmission

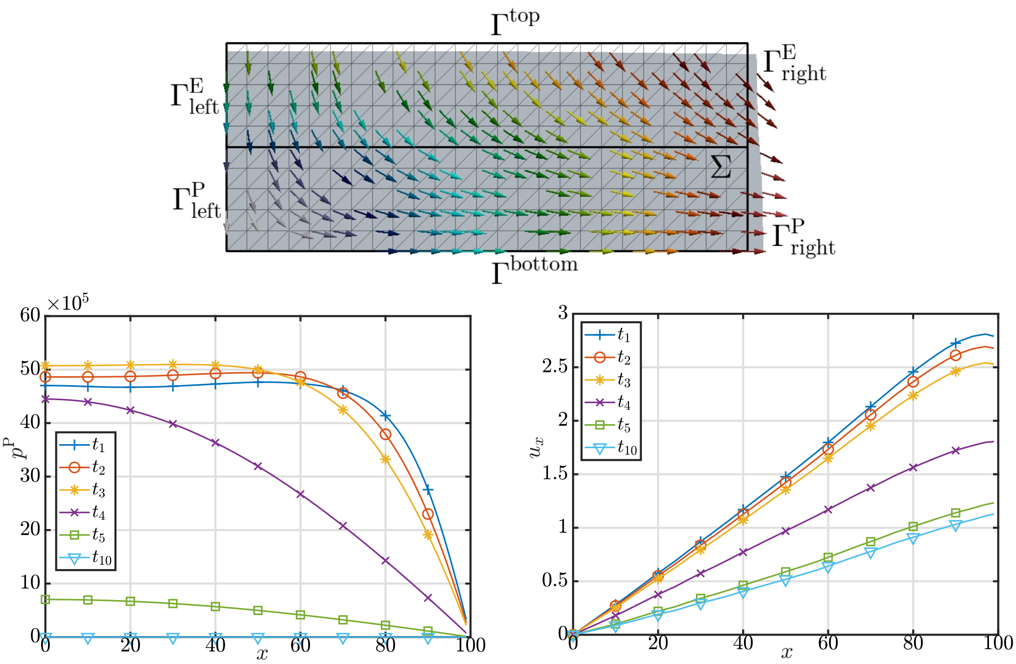

Fig. 3. *Test 2. Sample coarse mesh and domain/boundary configuration (top), and profiles of fluid pressure and x-displacement on Γ^{bottom} (bottom) at different times ($t_1 = 10^3$ s, $t_2 =$5e3 s, $t_3 = 10^4$ s, $t_4 = 10^5$ s, $t_5 =$5e5 s, $t_6 =$5e6 s) for the augmented Mandel problem.*

conditions, in the problem formulation, in the polynomial degree of the numerical schemes, and in mesh resolution), qualitatively, we observe the expected behaviour in fluid pressure profiles and motion patterns.

Test 3: poroelastic aquifer in 3D. Next we solve a 3D problem similar to that described in [15], where one is interested in determining deformation and fluid pressure distribution of the pay zone (a poroelastic aquifer region occupying $\Omega^{\text{P}} = (-225, 225) \times (-225, 225) \times (-30, 30)\,\text{m}^3$) surrounded by rock conforming the non-pay zone (an elastic, non-porous structure $\Omega^{\text{E}} = (-450, 450) \times (-450, 450) \times (-150, 150)\,\text{m}^3$). The scenario corresponds to coupled flow and poromechanics encountered in CO_2 sequestration in deep subsurface reservoirs. A localised source $s^{\text{P}}(x, y, z) = s_0 \exp(-(x - 225)^2 - (y - 225)^2)$ represents an injection zone of relatively small radius reaching the top corner of the pay zone. On the top surface of the pay rock, Γ^{top}, we assume zero traction, using the technique described in (5.2). On the remainder of Γ we impose the sliding condition

$$\boldsymbol{u} \cdot \boldsymbol{n} = 0 \qquad \text{on } \Gamma \setminus \Gamma^{\text{top}}.$$

Interface conditions are precisely as in (2.12), and we impose a smooth body load on the non-pay rock $\boldsymbol{f}^{\text{E}} = f_0(\sin(f_1 x)\sin(f_1 y), \cos(f_1 y)\cos(f_1 z), \frac{1}{2}\sin(f_1 z)\cos(f_1 x))^{\mathtt{t}}$. We now consider gravitational effects and take a relatively large permeability. The remaining parameters assume the values

$$s_0 = 1.8\text{e-}3, \quad f_0 = 10^{-3}, \quad f_1 = 7.5\text{e-}3, \quad \alpha = 0.8, \quad \rho = 1, \quad E^{\text{E}} = E^{\text{P}} = 3.4474\text{e+}9\,\text{Pa},$$
$$\nu^{\text{E}} = 0.45, \quad \nu^{\text{P}} = 0.2, \quad \xi = 10^{-3}\,\text{Pa s}, \quad \kappa = 9.869\text{e-}9\,\text{m}^2, \quad c_0 = 6.060\text{e-}5, \quad \boldsymbol{g} = (0, 0, -9.81)^{\mathtt{t}}.$$

The domain is discretised with a rather coarse tetrahedral mesh, and we employ a first-order scheme. From Figure 4 we observe an important deformation of the rock and the pay zone, as well as a fluid pressure propagating from the location of the injection well towards the opposite corner of the reservoir.

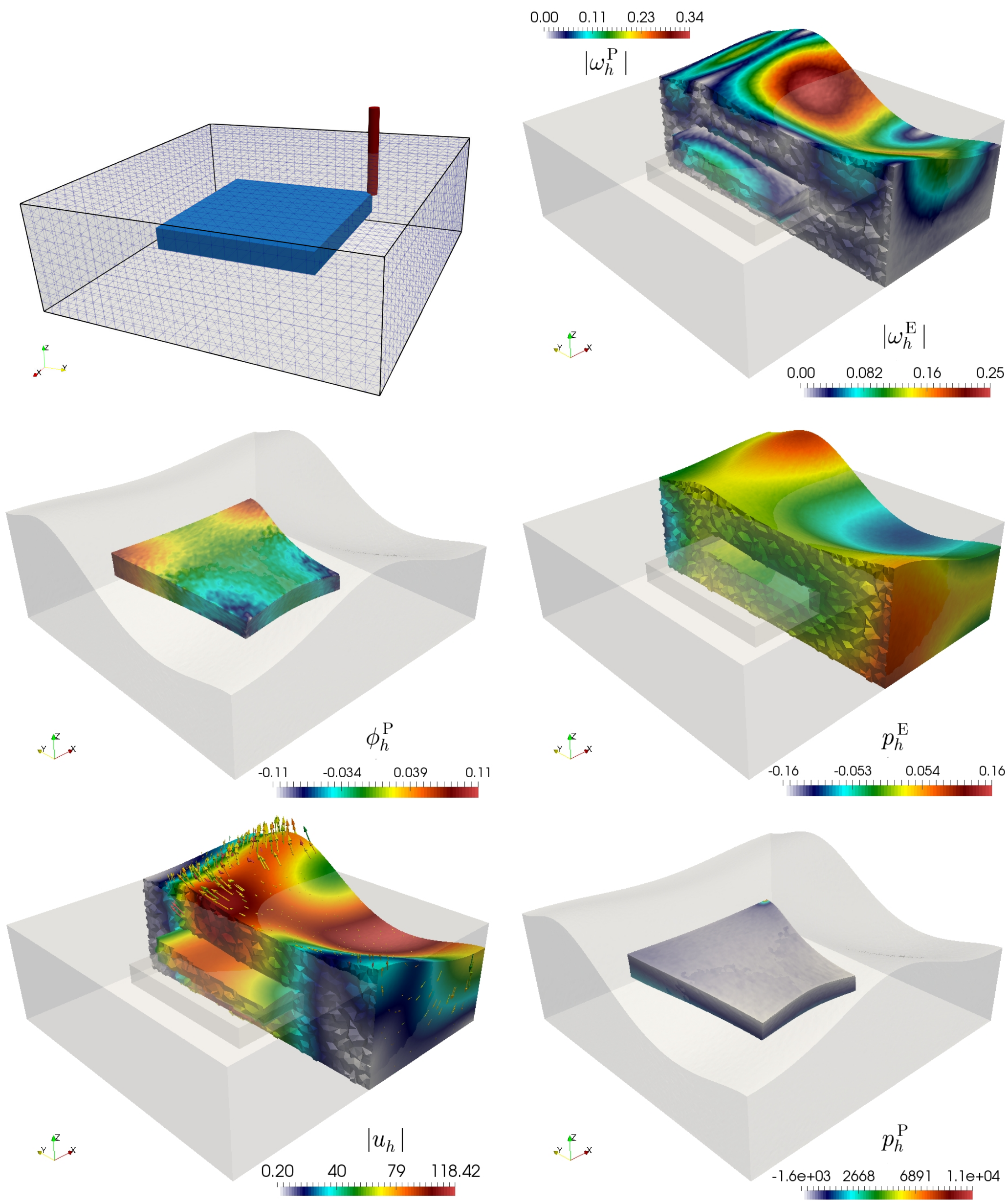

FIG. 4. *Test 3. Meshes associated with the confined reservoir Ω^{P} and the surrounding non-pay rock Ω^{E} (top left, sketching also the location of the injection well), and samples of approximate solutions generated with a first-order method.*

Test 4: coupling of tooth and periodontal ligament. We conclude with the simulation of distributed forces in a dentistry-oriented application. The problem set up is adapted from that in [9], where one considers the coupling between the tooth as elastic structure and the surrounding periodontal ligament regarded as a poroelastic material. In this case however we assume that the volume fractions in both regions coincide and that the fluid viscosity and density of each phase remain constant. The motivating example from [9] concentrates on determining displacement and stress behaviour of the composite material when a piezoelectric actuator applies an external load on the centre of the labial side of the crown of a two-rooted premolar in a porcine jawbone segment (the location is illustrated with a sphere in the first panel of Figure 5). A relatively

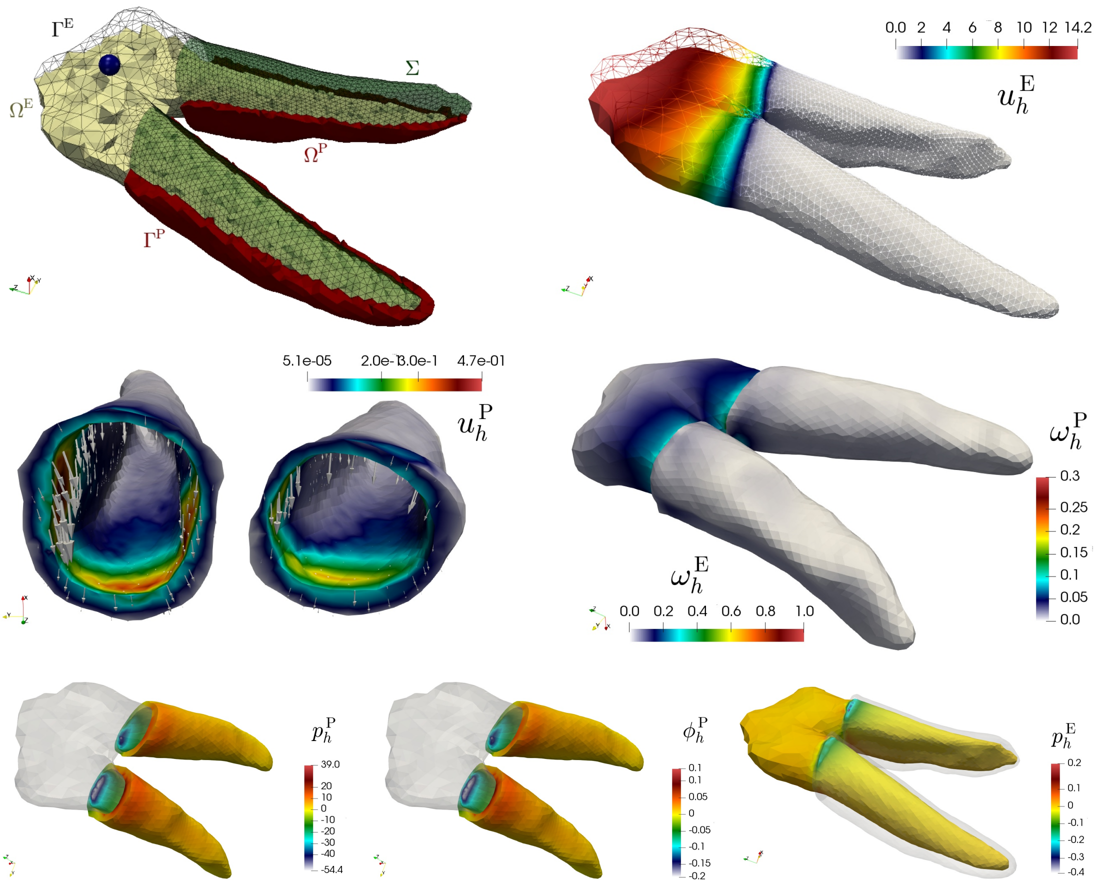

FIG. 5. *Test 4. Meshes associated with the periodontal ligament* Ω^{P} *and a porcine premolar specimen* Ω^{E} *(top left, sketching also the location of the applied load, 19 mm away from the root), and samples of approximate solutions generated with a second-order method.*

coarse tetrahedral mesh is used for both domains, and the boundary conditions are set in the following way. We assume that the external surface of the periodontal ligament, Γ^{P}, is in contact with the jawbone and therefore we set zero solid displacements and zero-flux conditions for the fluid pressure. On the visible part of the tooth, Γ^{E}, we impose the traction $\boldsymbol{t} = \frac{t_{\max}}{\lambda^{\mathrm{E}}+2\mu^{\mathrm{E}}}\chi|_{\mathrm{load}}$, where $\chi|_{\mathrm{load}}$ is the indicator function on a ball of radius 10 mm centred at $(200, 15, 60)$. And again the interface conditions on Σ are set as in (2.12). The body loads in both domains are $\boldsymbol{f}^{\mathrm{E}} = \frac{\rho^{\mathrm{E}}}{\lambda^{\mathrm{E}}+2\mu^{\mathrm{E}}}\boldsymbol{g}$ and $\boldsymbol{f}^{\mathrm{P}} = \frac{\rho^{\mathrm{P,s}}+\rho^{\mathrm{P,f}}}{\lambda^{\mathrm{P}}+\mu^{\mathrm{P}}}\boldsymbol{g}$, and the rest of the model parameters are set as

$$s_0 = 0, \quad c_0 = 10^{-3}, \quad t_{\max} = 0.016, \quad \alpha = 0.4, \quad \rho^{\mathrm{E}} = 6000, \quad \rho^{\mathrm{P,s}} = 1060, \quad \rho^{\mathrm{P,f}} = 1000,$$
$$E^{\mathrm{E}} = 2\mathrm{e}5, \quad E^{\mathrm{P}} = 2\mathrm{e}10, \quad \nu^{\mathrm{E}} = 0.3, \quad \nu^{\mathrm{P}} = 0.31, \quad \xi = 1, \quad \kappa = 10^{-6}\mathrm{mm}^2, \quad \boldsymbol{g} = (0, 0, -9.81)^{\mathtt{t}}.$$

Figure 5 reveals zones of concentrated solid pressure near the upper part of Σ, and also high gradients of fluid pressure are noticed in neighbouring areas, all consistently with the results reported in [9].

Acknowledgements. The authors express their sincere thanks to Marco Favino (Lausanne) for kindly providing the surface and volumetric meshes employed in Test 4, generated from micro-CT scanner images.

REFERENCES

[1] M. Alvarez, G. N. Gatica, and R. Ruiz-Baier, *A vorticity-based fully-mixed formulation for the 3D Brinkman-Darcy problem*, Computer Methods in Applied Mechanics and Engineering, 307 (2016), pp. 68–95.

[2] V. Anaya, Z. De Wijn, D. Mora, and R. Ruiz-Baier, *Mixed displacement-rotation-pressure formulations for linear elasticity*, Computer Methods in Applied Mechanics and Engineering, 344 (2019), pp. 71–94.

[3] L. Berger, R. Bordas, D. Kay, and S. Tavener, *Stabilized lowest-order finite element approximation for linear three-field poroelasticity*, SIAM Journal on Scientific Computing, 37 (2015), pp. A2222–A2245.

[4] F. Brezzi and M. Fortin, *Mixed and Hybrid Finite Element Methods*, Springer-Verlag, Berlin, 1991.

[5] M. Bukač, I. Yotov, R. Zakerzadeh, and P. Zunino, *Partitioning strategies for the interaction of a fluid with a poroelastic material based on a Nitsche's coupling approach*, Computer Methods in Applied Mechanics and Engineering, 292 (2015), pp. 138–170.

[6] S. Chaillat, M. Darbas, and F. Le Louër, *Approximate local Dirichlet-to-Neumann map for three-dimensional time-harmonic elastic waves*, Computer Methods in Applied Mechanics and Engineering, 297 (2015), pp. 62–83.

[7] C. D'Angelo and P. Zunino, *Robust numerical approximation of coupled Stokes' and Darcy's flows applied to vascular hemodynamics and biochemical transport*, ESAIM: M2AN, 45 (2011), pp. 447–476.

[8] G. de Boer, R. Hewson, M. Bryant, and D. Dowson, *An investigation into the contact between soft elastic and poroelastic bodies rotating under load*, Tribology - Materials, Surfaces & Interfaces, 11 (2017), pp. 193–201.

[9] M. Favino, C. Gross, M. Drolshagen, L. Keilig, J. Deschner, C. Bourauel, and R. Krause, *Validation of a heterogeneous elastic-biphasic model for the numerical simulation of the PDL*, Computer Methods in Biomechanics and Biomedical Engineering, 16 (2013), pp. 544–553.

[10] G. N. Gatica, *A Simple Introduction to the Mixed Finite Element Method. Theory and Applications*, Springer-Verlag, Berlin, 2014.

[11] G. N. Gatica, N. Heuer, and S. Meddahi, *On the numerical analysis of nonlinear twofold saddle point problems*, IMA J. Numer. Anal, 23 (2003), pp. 301–330.

[12] G.-M. Gie and J. P. Kelliher, *Boundary layer analysis of the Navier-Stokes equations with generalized Navier boundary conditions*, Journal of Differential Equations, 253 (2012), pp. 1862–1892.

[13] V. Girault, G. Pencheva, M. F. Wheeler, and T. Wildey, *Domain decomposition for poroelasticity and elasticity with DG jumps and mortars*, Mathematical Models and Methods in Applied Sciences, 21 (2011), pp. 169–213.

[14] V. Girault and P.-A. Raviart, *Finite Element Methods for Navier-Stokes Equations: Theory and Algorithms*, Springer Publishing Company, 1st ed., 1986.

[15] V. Girault, M. F. Wheeler, T. Almani, and S. Dana, *A priori error estimates for a discretized poro-elastic-elastic system solved by a fixed-stress algorithm*, Oil and Gas Science Technology, 74 (2019), p. 24.

[16] C. Goll, T. Wick, and W. Wollner, *DOpElib: Differential equations and optimization environment; a goal oriented software library for solving PDEs and optimization problems with PDEs*, Archive of Numerical Software, 5 (2017), pp. 1–14.

[17] P. Göransson, *Tailored acoustic and vibrational damping in porous solids – Engineering performance in aerospace applications*, Aerospace Science and Technology, 12 (2008), pp. 26–41.

[18] J. Heys, T. Manteuffel, S. McCormick, and J. Ruge, *First-order system least squares (FOSLS) for coupled fluid-elastic problems*, Journal of Computational Physics, 195 (2004), pp. 560–575.

[19] J. S. Howell and N. J. Walkington, *Inf–sup conditions for twofold saddle point problems*, Numerische Mathematik, 118 (2011), pp. 663–693.

[20] H. I. Ling and H. Liu, *Deformation analysis of reinforced soil retaining walls—simplistic versus sophisticated finite element analyses*, Acta Geotechnica, 4 (2009), pp. 203–213.

[21] A. Mikelić and M. F. Wheeler, *On the interface law between a deformable porous medium containing a viscous fluid and an elastic body*, Mathematical Models and Methods in Applied Sciences, 22 (2012), p. 1250031.

[22] R. Oyarzúa and R. Ruiz-Baier, *Locking-free finite element methods for poroelasticity*, SIAM Journal on Numerical Analysis, 54 (2016), pp. 2951–2973.

[23] S. Rani and S. Rani, *Axisymmetric deformation of a poroelastic layer overlying an elastic half-space due to surface loading*, Geophysical Journal International, 211 (2017), pp. 883–896.

[24] K. Rurkowska and S. Langer, *Coupling elastic-poroelastic material in structure-borne sound modeling*, The Journal of the Acoustical Society of America, 133 (2013), pp. 3446–3446.

[25] M. Serpilli, *Classical and higher order interface conditions in poroelasticity*, Annals of Solid and Structural Mechanics, in press (2019).

[26] T. Wick, A. H. Elsheikh, and M. F. Wheeler, *Parameter estimation for the coupled Biot-Lamé-Navier problem in subsurface modeling*, in 47th US Rock Mechanics / Geomechanics Symposium 2013, vol. 4, American Rock Mechanics Association, 2013, pp. 3000–3006.

Centro de Investigación en Ingeniería Matemática (CI²MA)

PRE-PUBLICACIONES 2019

2019-10 Andrea Cangiani, Mauricio Munar: *A posteriori error estimates for mixed virtual element methods*

2019-11 Alfredo Bermúdez, Bibiana López-Rodríguez, Rodolfo Rodríguez, Pilar Salgado: *Numerical analysis of a penalty approach for the solution of a transient eddy current problem*

2019-12 Javier A. Almonacid, Gabriel N. Gatica, Ricardo Ruiz-Baier: *Ultra-weak symmetry of stress for augmented mixed finite element formulations in continuum mechanics*

2019-13 Mario Álvarez, Gabriel N. Gatica, Ricardo Ruiz-Baier: *A mixed-primal finite element method for the coupling of Brinkman-Darcy flow and nonlinear transport*

2019-14 Marcelo Cavalcanti, Wellington Correa, Türker Özsari, Mauricio Sepúlveda, Rodrigo Véjar: *Exponential stability for the nonlinear Schrödinger equation with locally distributed damping*

2019-15 Ricardo Oyarzúa, Manuel Solano, Paulo Zuñiga: *A priori and a posteriori error analyses of a high order unfitted mixed-FEM for Stokes flow*

2019-16 David Mora, Iván Velásquez: *Virtual element for the buckling problem of Kirchhoff-Love plates*

2019-17 Veronica Anaya, Bryan Gomez-Vargas, David Mora, Ricardo Ruiz-Baier: *Incorporating variable viscosity in vorticity-based formulations for Brinkman equations*

2019-18 Felipe Lepe, David Mora: *Symmetric and non-symmetric discontinuous Galerkin methods for a pseudostress formulation of the Stokes spectral problem*

2019-19 Antonio Baeza, Raimund Bürger, Pep Mulet, David Zorío: *An efficient third-order WENO scheme with unconditionally optimal accuracy*

2019-20 Tomás Barrios, Edwin Behrens, Rommel Bustinza: *A stabilised mixed method applied to compressible fluid flow: The stationary case*

2019-21 Veronica Anaya, Zoa De Wijn, Bryan Gomez-Vargas, David Mora, Ricardo Ruiz-Baier: *Rotation-based mixed formulations for an elasticity-poroelasticity interface problem*

Para obtener copias de las Pre-Publicaciones, escribir o llamar a: Director, Centro de Investigación en Ingeniería Matemática, Universidad de Concepción, Casilla 160-C, Concepción, Chile, Tel.: 41-2661324, o bien, visitar la página web del centro: http://www.ci2ma.udec.cl




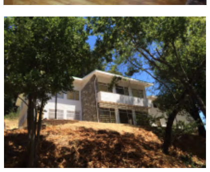
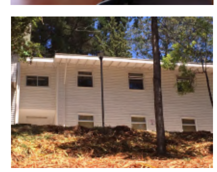

Centro de Investigación en
Ingeniería Matemática (CI^{2}MA)
Universidad de Concepción

Casilla 160-C, Concepción, Chile
Tel.: 56-41-2661324/2661554/2661316
http://www.ci2ma.udec.cl